Aus der Medizinischen Klinik und Poliklinik IV
der Ludwig-Maximilians-Universität München
Direktor: Prof. Dr. med. Martin Reincke

The regulation of XYLT1, the enzyme initiating glycosaminoglycan synthesis; An *in vitro* study with human immortalized fibroblasts with integrated reporter plasmid

Dissertation
zum Erwerb des Doktorgrades der Medizin
an der Medizinischen Fakultät der
Ludwig-Maximilians-Universität zu München

vorgelegt von

Marlena Christina Morhard

aus Eichstätt

2019

Mit Genehmigung der Medizinischen Fakultät

der Universität München

Berichterstatter:	Prof. Dr. med. Michael Fischereder
Mitberichterstatter:	PD Dr. med. Bärbel Lange-Sperandio
	Prof. Dr. med. Wolfgang Neuhofer
Mitbetreuung durch den promovierten Mitarbeiter:	Prof. Dr. rer. nat. Peter Nelson
Dekan:	Prof. Dr. med. dent. Reinhard Hickel
Tag der mündlichen Prüfung:	23.05.2019

Acknowledgements

I would like to thank

- Prof. Dr. Michael Fischereder and Prof. Dr. Peter Nelson, for mentoring me. I am grateful for their ideas and valuable comments on this thesis.
- Dr. Carsten Jäckel and my other fellow labmates, for sharing methods and ideas.
- The technical staff, for being helpful and friendly.
- My colleagues and friends, for companying me through the ups and downs of research life.
- My family: my parents, my brothers and my grandparents for their constant patience and support.
- My boyfriend Joakim, for providing me with unfailing support and continuous encouragement through the process of researching and writing this thesis.

Marlena Ch. Morhard

Eidesstaatliche Versicherung

Morhard, Marlena Christina

Ich erkläre hiermit an Eides statt,
dass ich die vorliegende Dissertation mit dem Thema

The regulation of XYLT1, the enzyme initiating glycosaminoglycan synthesis; An in vitro study with human immortalized fibroblasts with integrated reporter plasmid

selbständig verfasst, mich außer der angegebenen keiner weiteren Hilfsmittel bedient und alle Erkenntnisse, die aus dem Schrifttum ganz oder annähernd übernommen sind, als solche kenntlich gemacht und nach ihrer Herkunft unter Bezeichnung der Fundstelle einzeln nachgewiesen habe.

Ich erkläre des Weiteren, dass die hier vorgelegte Dissertation nicht in gleicher oder in ähnlicher Form bei einer anderen Stelle zur Erlangung eines akademischen Grades eingereicht wurde.

München, 24.05.19	Marlena Christina Morhard
_____	_____
Ort, Datum	Unterschrift Doktorandin

Abstract

Several studies suggest that sodium is not only linked to extracellular fluids, but is also found in considerable amounts in other sites of the body including skin, muscle and arteries, where it is stored osmotically inactive, presumably bound to glycosaminoglycans. In a recent study, a correlation between tissue sodium concentrations, glycosaminoglycan content and the expression of XYLT1, the enzyme initiating glycosaminoglycan synthesis, was found. Thus, the aim of the present *in vitro* study was to investigate the potential regulation of XYLT1 expression in human fibroblast cells, in order to gain further insight into potential regulatory mechanisms of tissue sodium storage. We hypothesized that XYLT1 expression can be actively induced by external stimuli.

As a tool for internal control of successful stimulation, human immortalized dermal fibroblasts were stably transfected with pathway specific reporter plasmids (TGF-β/SMAD and NFAT5, respectively), with a fluorescent protein read-out (Gaussia Luciferase), allowing the monitoring of pathway activation status in response to different experimental conditions. XYLT1 expression was quantified by real-time PCR.

We observed significant induction of XYLT1 expression by treatment with TGF-β1 and TGF-β3. Media with hypertonic sodium, elevated Vasopressin, Endothelin-1 and FGF23 concentrations, respectively, did not have significant effects on XYLT1 expression.

In conclusion, we established functioning systems to monitor pathway activation status as internal control of treatment with TGF-β and hypertonic sodium. Our data support the hypothesis that XYLT1 is actively regulated by TGF-β, which strengthens the theory that there is active regulation of water-free sodium storage. To investigate this theory further, we suggest *in vitro* quantification of sodium concentration and glycosaminoglycan content relative to XYLT1 expression as a next step.

Kurzfassung

Etliche Studien weisen darauf hin, dass Natrium im Körper nicht nur an extrazelluläre Flüssigkeit gebunden ist, sondern auch in bedeutenden Mengen in anderen Bereichen des Körpers, wie Haut, Muskeln und Arterien, existiert, wo es - vermutlich an Glykosaminoglykane gebunden - osmotisch inaktiv gespeichert wird. In einer kürzlich durchgeführten Studie wurde eine positive Korrelation zwischen Natriumkonzentrationen in Gewebe, Glykosaminoglykan-Gehalt und der Expression von XYLT1, dem Schlüsselenzym der Glykosaminoglykan-Synthese, gefunden. Das Ziel dieser Arbeit war deshalb, die Regulation von XYLT1 näher zu untersuchen, um bessere Einsicht in die regulatorischen Mechanismen von Gewebe-Natriumspeichern zu erlangen. Unsere Hypothese war, dass XYLT1-Expression durch externe Stimuli wie TGF-β aktiv induziert werden kann.

Für die Stimulationsexperimente wurde folgendes *in vitro* Zellkulturmodel etabliert: Humane dermale Fibroblasten wurden stabil mit TGF-β/SMAD oder NFAT5 Reportertransgenen transfiziert, um mittels eines fluoreszenten Reporterproteins den Aktivitätsstatus des jeweiligen Signalwegs unter verschiedenen experimentellen Bedingungen verfolgen zu können. Dies ermöglichte eine interne Kontrolle für erfolgreiche Stimulation. Nach Inkubation mit unterschiedlichen Stimuli wurde XYLT1 Expression mittels quantitativer Echtzeit-PCR bestimmt.

Als Ergebnis zeigte sich eine starke Induktion der XYLT1 Expression nach Stimulation mit TGF-β1 und TGF-β3. Inkubation mit erhöhten Konzentrationen von Natrium, Vasopressin, Endothelin-1 oder FGF23 hatte dagegen keinen Effekt auf XYLT1 Expression, im Vergleich zur Kontrolle.

Zusammenfassend wurde in dieser Arbeit ein funktionierendes System zur Überwachung des Aktivitätsstatus von Signalwegen etabliert, das hier als Kontrolle für Stimulation mit TGF-β und hypertonem Natrium diente. Die Ergebnisse der Stimulationsexperimente unterstützen die Hypothese, dass XYLT1 aktiv durch TGF-β reguliert wird. Dies stärkt die Theorie, dass eine aktive Regulation der osmotisch inaktiven Gewebe-Natriumspeicher existiert. Um diese Theorie zu belegen, erscheint die Quantifizierung von Gewebe-Natriumkonzentration und Glykosaminoglykan-Gehalt *in vitro* relativ zu XYLT1 Expression ein wichtiger nächster Schritt.

Table of contents

Figures

Tables

Abbreviations

	Abbreviation	Description
A	ACTH	Adrenocorticotropic hormoe
	ADH	Antidiuretic hormone
	ATPase	Adenosintriphosphatase
	AVP	Arginine vasopressin
B	Bp	Base pair(s)
C	cDNA	Complementary DNA
	CKD	Chronic kidney disease
	CHPF	Chondroitin polymerizing factor
	CHSY1	Chondroitin sulfate synthase 1
	CO_2	Carbon dioxide
	C_p	Crossing point-qPCR cycle
D	dATP	Deoxyadenosine triphosphate
	dCTP	Deoxycytidine triphosphate
	dGTP	Deoxyguanosine triphosphate
	DMEM	Dulbecco's Modified Eagle's Medium
	DMSO	Dimethyl sulfoxide
	DNA	Deoxyribonucleic acid
	DNAse	Deoxyribonuclease
	dNTPs	Deoxyribonucleotide triphosphates
	DPBS	Dulbecco's Phosphate Buffered Saline
	dsDNA	Double stranded DNA
	DTT	Dithiothreitol
	dTTP	Deoxythymidine triphosphate
E	E.coli	Escheria coli
	ET-1	Endothelin-1

	EDTA	Ethylenediaminetetraacetic acid
F	FCS	Fetal calf serum
	FGF23	Fibroblast growth factor 23
	FGFR	Fibroblast growth factor receptors
	FGFR4	Fibroblast growth factor receptor 4
	FW	Forward
G	GAG	Glycosaminoglycan(s)
H	H_20	Water
J	JIP4	N-terminal kinase-interacting protein-4
K	Kb	Kilobase
L	Lb	Lysogeny broth
M	mM	Mili molar
	MAPK	Mitogen-activated protein kinase
	$MgCl_2$	Magnesium chloride
	23Na-MRI	23Na magnetic resonance imaging
	Na^+	Sodium ion
	NaCl	Sodium chloride
	NFAT5	The nuclear factor of activated T cells-5
	Nf-κB	Nuclear factor kappa-light-chain-enhancer of activated B-cells
P	PCR	Polymerase chain reaction
	ph	Potential of hydrogen
	P/S	Penicillin/Streptomycin
Q	qPCR	Quantitative polymerase chain reaction
R	RLU	Relative light units
	RNA	Ribonucleic acid
	RNAse	Ribonuclease
	RNAsin	Ribonuclease inhibitor

	RT-PCR	Reverse transcription polymerase chain reaction
	RV	Reverse
S	SARA	SMAD anchor for receptor activation
	SOC	Super optimal broth
T	Taq	Thermos aquaticus
	TBE	Tris-borate-EDTA
	TGF-β	Transforming growth factor β
	T_m	Melting temperature
U	UV	Ultraviolet
V	V	Volt
	VEGF-C	Vascular endothelial growth factor C
X	XYLT1	Xylosyltransferase 1

1 Introduction

1.1 Biological role of sodium

Sodium is an essential electrolyte in humans and animals. As the major cation in extracellular fluids, it plays an important role in the regulation of blood pressure and acid-base balance and in maintenance of fluid balance with its ability to attract and hold water. Moreover, it is a central substance for building up membrane potential through the Na^+/K^+ ATPase, allowing muscles and nerves to carry electrical impulses. The concentrations of sodium in the extracellular fluid are normally maintained within a narrow range around 135-145 mmol/L, by the hypothalamic-renal feedback systems. However, serum sodium disturbances can develop by imbalanced elimination or ingestion of sodium. The resulting hyponatremia or hypernatremia can cause variable symptoms and can, in the worst case, be lethal, therefore they often require medical attention.

1.2 Current paradigm regarding sodium handling in humans

The common understanding of sodium handling is, as described in most textbooks, that sodium to a large extent, is linked to extracellular body fluids, perhaps with a minor component stored in bone tissue. It is generally assumed that serum sodium regulation functions as follows: Increase of dietary sodium intake leads to elevation of plasma osmolality, triggering thirst and the secretion of antidiuretic hormone while reducing aldosterone levels. Greater water intake combined with increased water retention lead to augmentation of circulating fluid volume and weight. Approximate 2-4 days are required to establish a new steady-state, in which urinary sodium excretion and sodium intake match (Walser, 1985). When dietary sodium intake is reduced, the mechanisms are reversed. Without doubt, this model is applicable in most clinical cases. However, there are extremes in the clinical spectrum that cannot be fully explained by the common understanding of sodium homeostasis. For example, there are observations of patients with severe kidney failure with increasing serum sodium levels, despite dialysis, and low sodium input. In the opposite extreme, some anuric patients are to a certain extent, able to compensate for sodium loading. These observations suggest that sodium can be stored elsewhere in the body otherthan in extracellular fluids, and that sodium balance is a more complex biological process than previously assumed.

1.3 Paradigm shift? - Water-free storage of sodium

The presence of a slow exchangeable pool of body sodium was already hypothesized 60 years ago (Farber, 1960), (Streeten, Rapoport, & Conn, 1963), but eventually lost favor and was not actively pursued. However, in the last 20 years, the interest in sodium storage has been renewed.

A detailed balance study in 2000, in which healthy men were given high sodium intakes, contradicted the equilibrium theory of sodium balance by showing no increase of total body water and no change in body weight despite increased total body Na^+ (Heer, Baisch, Kropp, Gerzer, & Drummer, 2000). In another balance study in a long-term space flight simulation, sodium gain exceeded weight gain towards the end of isolation, suggesting sodium accumulation in an osmotically inactive form. As a potential reservoir, bone, dense connective tissue or cartilage was proposed (Titze, Maillet, et al., 2002). Recent studies with non-invasive ^{23}Na-MRI measurements of Na^+ content in tissue support this observation by demonstrating increased tissue sodium concentrations in skin and muscle in patients with primary hyperaldosteronism without apparent fluid retention or significant changes in Na^+ concentration in serum (C. Kopp et al., 2012). The phenomenon of osmotically inactive Na^+ storage has also been confirmed experimentally in animals: A study in Sprague-Dawley rats showed that Na^+ accumulated in skin after high NaCl diet, concluding that osmotically inactive Na^+ storage takes place largely in the skin (Titze et al., 2003).

However, the mechanisms responsible for tissue Na^+ storage are not fully understood. Various studies suggest incorporation into glycosaminoglycans (GAGs) as a potential site of sodium storage. In rats exposed to sodium loading, increasing skin Na^+ coincided with significant increases in glycosaminoglycan expression on Western blot of the skin (Titze et al., 2004). Long-term salt deprivation, conversely, resulted in reduced negatively charged skin glycosaminoglycan content and release of Na^+ from the skin reservoir (Schafflhuber et al., 2007). The idea of sodium-proteoglycan binding was in fact found already four decades ago, based on GAG measurements in the skin of Wistar rats with different salt loads (Ivanova, Archibasova, & Shterental, 1978) and was also described in binding studies in glycosaminoglycan rich tissues (Mobasheri, 1998).

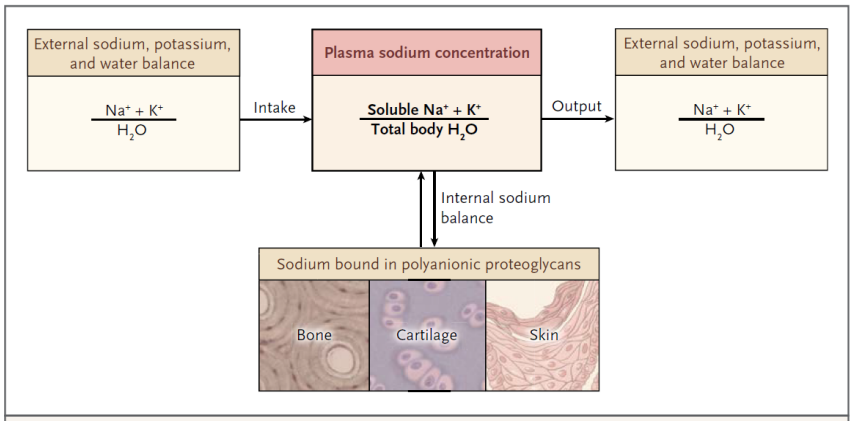

Figure 1: Sodium balance

Internal balance through exchange between sodium linked to body water and sodium that is bound to proteoglycans in bone, cartilage and skin. Image adapted from Sterns (2015, p. 2).

Taken together, sodium is most likely stored water free in tissue and potentially bound to glycosaminoglycans. However, the regulation of this storage, and its role in physiology and disease, are not well understood.

1.4 The findings in "sodium storage in human tissues is mediated by glycosaminoglycan expression" as base for this work

Most recently, a human study was performed at our institute, supporting the theory that GAG expression mediates sodium storage in human tissues, including skin, muscles and arteries (Fischereder et al., 2017). The findings of this study, described in the following, gave origin to further questions regarding the regulation of GAG expression, which lead to the present work. In this study, 27 dialysis patients, mostly recipients of living kidney transplants, and 21 healthy transplant donors, were included. During surgery, tissue samples of abdominal skin, muscle and arteries were taken. The Na^+ content in the tissue $[Na]_T$ was then measured by inductively coupled plasma-optical emission spectroscopy. Glycosaminoglycan content was assessed in skin, muscle and arterial samples by standardized Alcain Blue-PAS staining (Fischereder et al., 2017). To investigate regulation of GAG-synthesis, expression of genes involved in GAG-synthesis was analyzed by RT-PCR in the respective biopsies. The data showed no difference in $[Na]_T$ between dialysis patients and healthy controls, thus supporting the results of previous studies (Dahlmann et al., 2015), but a high interindividual variability of $[Na]_T$ was seen. However, there was an intraindividual correlation of $[Na]_T$ found for skin, artery and muscle, significantly highest in arteries and significantly lowest in muscle (Fischereder et al., 2017). Furthermore, $[Na]_T$ correlated significantly with glycosaminoglycan content of the tissue and with the expression of Xylosyltransferase 1 (XYLT1), the enzyme catalyzing the first step in biosynthesis of GAGs (Fischereder et al., 2017).

The findings of the study support the relevance of glycosaminoglycan expression in water-free sodium storage in skin, muscle and arteries. Furthermore, Fischereder et al. (2017, p. 6) hypothesized that glycosaminoglycan expression and $[Na]_T$ is actively regulated, raising the question as to which biologic mechanisms trigger XYLT1 expression and GAG synthesis. In the *in vivo* study, the XYLT1 expression, assayed with RT-PCR, correlated with calculated osmolality and serum-phosphate levels. However, *in vitro* experiments with immortalized human fibroblasts did not show the same correlation. On the other hand, treatment with the pleiotropic cytokine transforming growth factor β (TGF-β) *in vitro* led to increased XYLT1 expression (Fischereder et al., 2017).

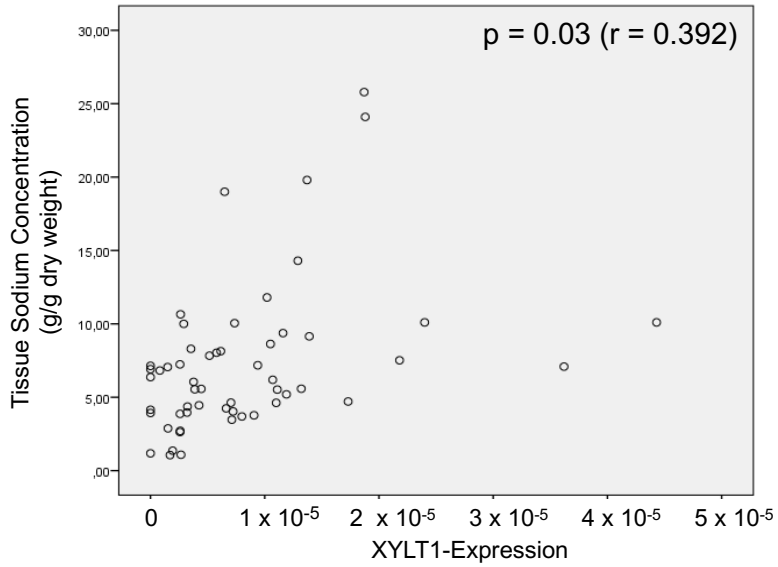

Figure 2: Tissue sodium concentrations correlate with XYLT1-Expression

Tissue sodium concentrations measured in muscles and arteries correlated with XYLT1 expression of the respective biopsy. Image adapted from Fischereder et al. (2017, p. 5).

1.5 Biology of glycosaminoglycans

In order to better understand how glycosaminoglycans (GAGs) may function as a potential site for sodium storage, it is essential to gain insight into the complex biology of GAGs, especially their synthesis and function. Glycosaminoglycans are linear chains of sulfated polysaccharides and composed of alternating copolymers of amino sugars (glucosamine that is N-acetylated, N-sulfated or N-acetylgalactosamine) and either an uronic acid (glucorunic acid or iduronic acid) or galactose. GAGs are produced by virtually all mammalian cells (Lindahl et al., 2015, pp. 1-4). Owing to the presence of acidic sugar residues and/or sulfate groups along the GAG chains, GAGs possess a highly negative charge (Prydz & Dalen, 2000, p. 1). Linear sulfated GAGs are classified in four major subclasses based on their disaccharide composition and sulfation: Chrondroitin sulfate (CS), dermatan sulfate (DS), heparan sulfate (HS) and heparin (Sugahara & Kitagawa, 2000). The sulfated GAG chains are covalently attached to a core protein to form proteoglycans. The type of GAG chain that becomes attached depends on the structure of the core protein and the environment of the Golgi apparatus, the place where GAGs are polymerized and subsequently sulfated. GAG chains are linked to the respective core protein through the common GAG-protein

linkage region GlcA-Gal-Gal-Xyl-O-Ser (Lindahl et al., 2015, p. 4). The biosynthesis of GAGs is initiated by the formation of this linkage region. The key enzyme of GAG chain initiation in proteoglycans is Xylosyltransferase (XYLT), which catalyzes the transfer of D-xylose from UDP-D-xylose to specific serine residues of the core protein (Muller et al., 2005, p. 1). The activity of XYLT is thought to be rate-limiting, which makes it an important potential regulatory factor in GAG biosynthesis (Stoolmiller, Horwitz, & Dorfman, 1972, p. 8). There exist two XYLT family members in mammals, xylosyltranferase 1 (XYLT1) and xylosyltranferase 2 (XYLT2). XYLT1 was shown to have enzymatic activity, while XYLT2 did not show enzymatic activity *in vitro*; its function is, for the most part, unknown (Brunner, Kolarich, Voglmeir, Paschinger, & Wilson, 2006). However, a study in Chinese hamster ovary cells suggests a significant role for XYLT2 in proteoglycan biosynthesis and hypothesized that the cell type may determine which xylosyltransferase family member is utilized (Cuellar, Chuong, Hubbell, & Hinsdale, 2007, p. 5).

After their synthesis, proteoglycans are transported from the Golgi apparatus to their site of function. They are the major component of the extracellular matrix, and are also found at the cell surface and in intracellular organelles. GAGs as part of proteoglycans are known to have diverse functions. They are, amongst others, involved in cell adhesion and cytokine action and play an important role in the control of growth and differentiation. They also provide structural integrity to connective tissue and cells (Kuhn et al., 2001). What makes GAGs interesting for this study, is their highly negative charge, which may give them the ability to incorporate Na^+, by attracting the positively charged Na^+ ions to leave their hydrated state (Titze et al., 2004).

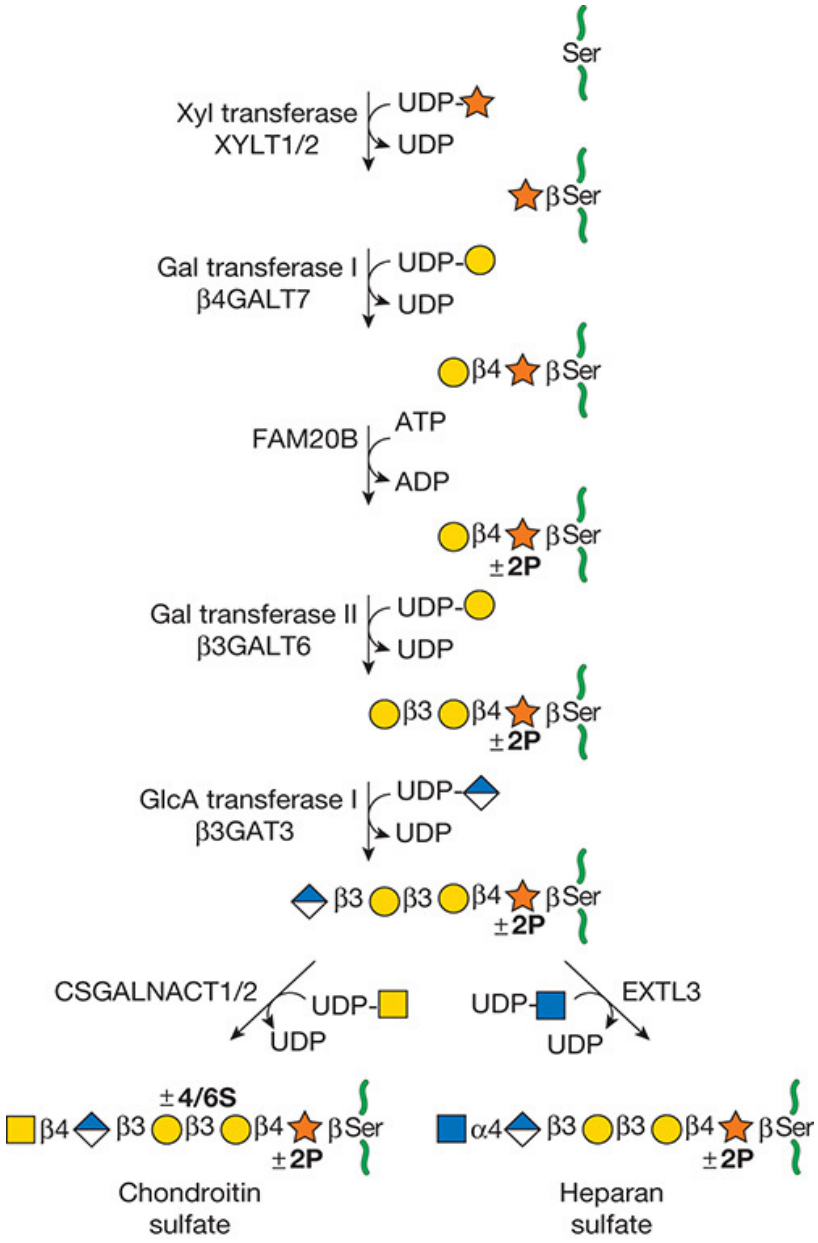

Figure 3: Biosynthesis of GAGs

Initiation of the biosynthesis of chondroitin sulfate (left chain) and heparan sulfate (right chain) by the key enzyme XYLT. Image adapted from Lindahl, Couchman, Kimata, and Esko (2015, p. 12).

1.6 Transforming growth factor β and its role in renal disease

As transforming growth factor β (TGF-β) has been suggested to influence GAG synthesis and is known to play a role in kidney disease, it appears to be a relevant subject when discussing the potential regulation of non-osmotic sodium storage, and is addressed in more detail in the following sections of the thesis. TGF-β and related factors are shown to be essential for the regulation of diverse biological processes. They play an important role during embryogenesis, in the homeostasis of most human tissue, regulation of immune response and wound healing. Moreover, they are involved in several pathologies including cancer, developmental disorders and tissue fibrosis (Finnson, McLean, Di Guglielmo, & Philip, 2013). Though the TGF-β superfamily is composed of a large number of structurally related polypeptide growth factors, this summary will focus solely on the TGF-β subfamily. There exist three isoforms of TGF-β in mammalian tissues, TGF-β1, TGF-β2 and TGF-β3, which share more than 70% of sequence similarity, but are known to have partly different biological activities (Mittl et al., 1996). The most abundant isoform is TGF-β1, which is ubiquitously expressed. TGF-β is synthesized as a precursor protein and secreted as a latent TGF-β complex, remaining inactivated in the ECM until its activation by protease, acidlase balance, heat, thrombospondin-1, reactive oxygen species and integrin (Khalil, 1999).

It is well known that TGF-β contributes to pathophysiology of many renal diseases, including diabetic nephropathy (Ziyadeh, Sharma, Ericksen, & Wolf, 1994), functioning as a key mediator in the pathogenesis of renal fibrosis (J. B. Kopp et al., 1996). Once activated, TGF-β induces elevated production of extracellular matrix proteins, leading to conditions associated with kidney fibrosis, such as glomerulosclerosis and tubulointerstitial fibrosis (Loeffler & Wolf, 2014). This pro-fibrotic effect has also been confirmed by the findings that therapeutic targeting of TGF-β can reduce renal injury (Chen et al., 2003). However, the potential clinical success of these interventions is at present uncertain, as recent studies in TGF-β transgenic mice have demonstrated that TGF-β not only triggers renal fibrosis, but, also, when present as a latent complex, induces anti-inflammatory effects, and thus preventing renal inflammation (Huang, Chung, Wang, Lai, & Lan, 2008). An inhibition of inflammation was also associated with an increase in SMAD7, an inhibitory version of the SMAD transcription factor family (detailed below), that is activated by TGF-β signaling as negative feedback mechanism loop (Wang et al., 2005).

These observations indicate a pleiotropic activity of TGF-β in renal disease, suggesting diverse roles for activated TGF-β (pro-fibrotic) and latent TGF-β (anti-inflammatory) (Sureshbabu, Muhsin, & Choi, 2016). The multifunctionality of TGF-β and its role in kidney disease were investigated further in this study.

1.7 Relevant signaling pathways

1.7.1 TGF-β/SMAD signaling

Activated TGF-β exerts its biological effects, as well as its pro-fibrotic effect in renal disease, by activating the canonical SMAD signaling pathway (Kubiczkova, Sedlarikova, Hajek, & Sevcikova, 2012). Activated TGF-β binds to the transmembrane receptor TGF-β receptor type II and brings it together with the TGF-β receptor type I receptor, both serine/theorine kinase receptors, forming a functional heterodimer. This leads to recruitment and activation of SMAD family transcription factors: Via the function of SMAD anchor for receptor activation (SARA) as an adaptor protein, phosphorylation of the intracellular regulatory R-SMAD proteins SMAD2/3 takes place. In their phosphorylated form, R-SMAD proteins have a high affinity to bind Co-SMADS, here SMAD4, that cooperate during signaling. The resulting complex of R-SMADs and Co-SMAD is then transported into the nucleus of the recipient cell to modulate gene transcription of target genes (Massague, 1998).

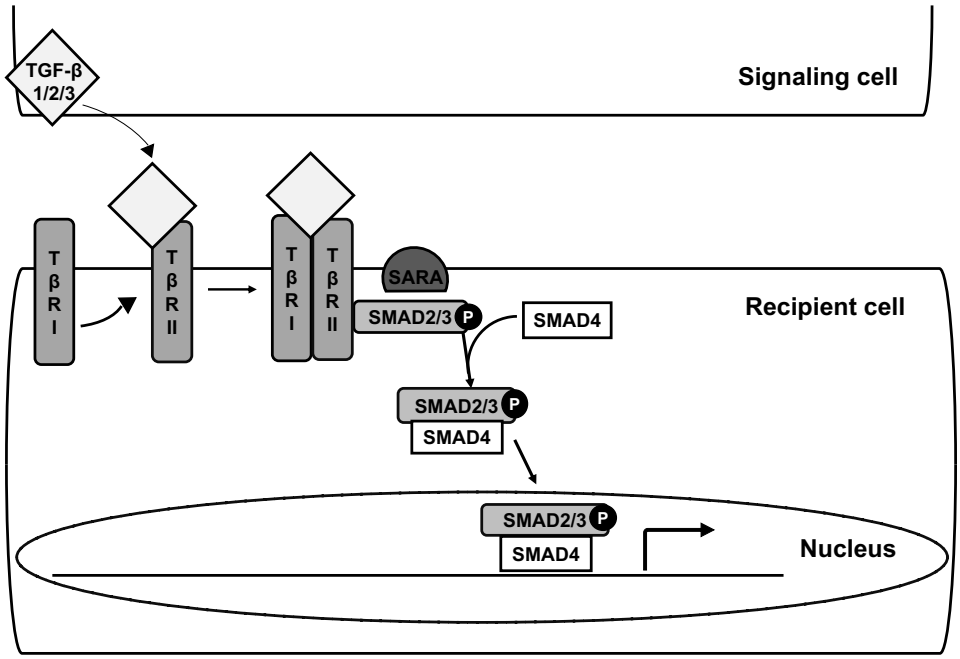

Figure 4: TGF-β driven SMAD activation pathway

Binding of the activated ligands TGF-β1/2/3 to TβRII brings together TβRI and TβRII, both serine/threonine protein kinases. One of these kinases phosphorylates the other, which in turn triggers the phosphorylation of the R-SMADS SMAD2/3. Phosphorylated R-SMADS bind to co-SMAD4 and the complex is transported into the nucleus where it regulates gene expression. TβRI= TGF-β type II receptor, TβRII= TGFβ type II receptor, SARA= SMAD anchor for receptor activation, P= phosphorylation.

TGF-β signaling leads to activation of inhibitory SMADs (I-SMADS), e.g. SMAD7, which function in a negative feedback loop. Importantly, a number of non-canonical TGF-β pathways have been identified, which may function independently of SMAD (Derynck & Zhang, 2003). The factors driving noncanonical activation of the pathway are not well characterized.

1.7.2 Hyperosmotic stress and NFAT5-mediated osmotic response activation

As steady state XYLT1 mRNA expression was shown to correlate with the calculated osmolality *in vivo* (refer to 1.4), biologic mechanisms involved in the osmotic stress response will be addressed in this, and following paragraphs, as they may be relevant for regulation of sodium storage. Elevation of extracellular sodium levels leads to hyperosmotic stress and can be harmful to cells. It can result in cell deformation, a disturbance in cellular function and inhibition of cellular proliferation. The Nuclear Factor of Activated T Cells- 5 (NFAT5), also known as tonicity enhancer binding protein (TonEBP), is a transcription factor that protects mammalian cells from hyper-osmotic stress by stimulating the transcription of osmoprotective genes (Miyakawa, Woo, Dahl, Handler, & Kwon, 1999). NFAT5 is the latest member of the so called *Rel* family of transcription factors, which in addition to NFAT5, includes the other Nuclear Factors of Activated T cells (NFAT) 1-4 and Nf-κB. Although the NFAT proteins share a similar structure, NFAT5 differs greatly from the other NFAT proteins: It does not possess a calcineurin binding domain, as the proteins NFAT1-4 do, but instead is highly sensitive for NaCl-induced hypertonicity (Aramburu et al., 2006). Various studies showed that NFAT5 has an important osmoprotective function in the kidney, where cells are physiologically exposed to hyperosmolarity, thus ensuring proper function of the renal medulla during antidiuresis (Christoph, Beck, & Neuhofer, 2007). However, its function is not limited to the renal medulla, since NFAT5 is expressed in virtually all tissues, and plays an important role for these tissues to survive and function properly in hypertonic environments (Trama, Lu, Hawley, & Ho, 2000). Although the exact molecular events leading to regulation of NFAT5 in response to hyper-osmotic stress are not fully understood, more than a dozen protein and lipid kinases have been identified in this context (Zhou, 2016). The following mechanism has been suggested to describe NFAT5 activation: The Guanine Nucleotide Exchange Factor Brx, located near the plasma membrane, responds to osmotic stress with activation of Rho-type small G-proteins and stimulates the MAPK cascade by interacting with c-Jun N-terminal kinase-interacting protein-4 (JIP4), a p38 MAPK-specific scaffold protein. Then, a complex of JIP4 with downstream kinases MKK3 and MKK6 is formed, which leads to activation of p38 mitogen-activated protein kinases (p38 MAPK), which in turn stimulate the transcription factor NFAT5 (Kino et al., 2009). Subsequently, NFAT5 induces osmoprotective gene products, that allow cells to adapt to the hypertonic environment.

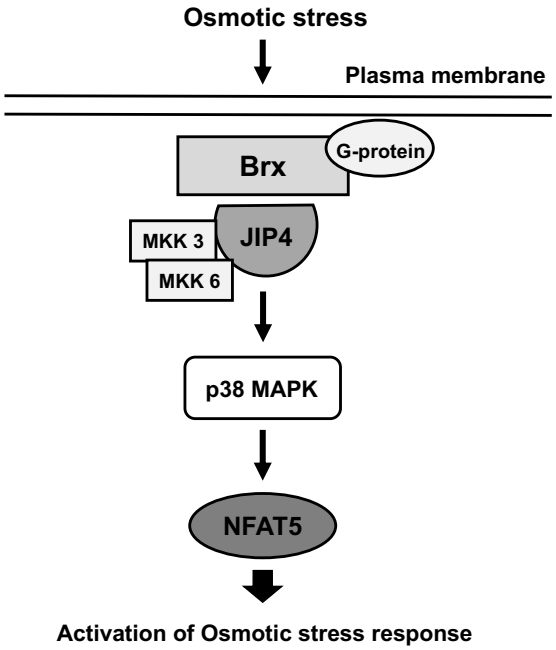

Figure 5: NFAT5 mediated osmotic response activation

Hyperosmolar environment leads to a physical interaction between Brx and JIP4 and the activation of Rho type small G-proteins. A complex of JIP4 and the downstream kinases MKK3 and MKK6 activates p38 MAPK, which in turn induces NFAT5 expression leading to activation of osmotic stress response. BRx= Guanine Nucleotide Exchange Factor Brx, JIP4= c-Jun N-terminal kinase-interacting protein-4, p38 MAPK= p38 mitogen-activated-protein kinases, NFAT5= Nuclear Factor of Activated T Cells-5.

In addition to its well-known osmoprotective function, NFAT5 also regulates genes that are not obviously associated with hypertonic stress (Neuhofer, 2010, p. 2). Amongst others, the induction of NFAT5 in macrophages of the skin was shown to induce the expression of the vascular endothelial growth factor C (VEGF-C), leading to increased lymphangiogenesis (Jantsch, Binger, Muller, & Titze, 2014). Interestingly, NFAT5 induction was also shown to positively regulate β-1,3 Glucuronosyltransferase-I (GlcAT-I), an enzyme important in glycosaminoglycan synthesis, in nucleus pulposus cells (Hiyama et al., 2009). These findings suggest biological importance of NFAT5 beyond its function in osmoprotection.

1.8 Endocrine regulators in sodium and mineral homeostasis

As stated above, various mechanisms involved in the osmotic stress response may have an effect on the regulation of sodium storage through their influence on GAG synthesis. A selection of endocrine regulators in sodium and mineral homeostasis are discussed below.

1.8.1 Arginine vasopressin (AVP)

Arginine vasopressin (AVP), also termed antidiuretic hormone (ADH), is an important mediator linked to maintaining the stability of the body fluid osmolality, in addition to other physiological functions. It is synthesized as a prohormone in the hypothalamus and stored in the posterior pituitary gland. AVP is released from the pituitary gland as a physiological response to increased plasma osmolality or hypovolemia (Kam, Williams, & Yoong, 2004). Once secreted, it has a strong antidiuretic effect in the kidney by acting through the renal vasopressin receptor V2 in cells of the collecting duct, leading to mobilization of aquaporin water channels, and thus increased water reabsorption. As a reasonable complimentary effect, AVP has vasoconstrictive effects mediated by vasopressin receptor V1 in vascular smooth muscle (Barberis, Mouillac, & Durroux, 1998), which helps to maintain blood pressure in situations with hypovolemia. Vasopressin receptor V1 is also expressed in cardiac myocytes, brain, testis, liver and renal medulla. Additionally, vasopressin promotes ACTH release by binding to the pituitary receptors V3 and may play a role in central control of circadian rhythm and thermoregulation (Mieda et al., 2015).

1.8.2 Endothelin

Endothelin is a cell derived peptide that functions as the most powerful vasoconstrictor known. There exist three isoforms in mammalian cells, ET-1, ET-2 and ET-3, though this summary will focus on Endothelin-1 (ET-1), which is produced in vascular endothelium as well as renal epithelial cells (Kohan, Inscho, Wesson, & Pollock, 2011). It was shown that ET-1 is involved in the regulation of arterial pressure and in Na^+ homeostasis during conditions of elevated salt intake (Pollock & Pollock, 2001), most likely through controlling salt handling within the kidney. Furthermore, recent data showed that ET-1 leads to facilitation of Na^+ movement through the skin interstitium during sodium loading (Speed et al., 2015, pp. 5-6).

1.8.3 Fibroblast growth factor 23

The protein fibroblast growth factor 23 (FGF23) is a member of the fibroblast growth factor (FGF) family and plays an important role in phosphate and vitamin D homeostasis (Kiela & Ghishan, 2009, pp. 3-4). It is produced in bone and its primary physiological function is associated with stimulation of urinary phosphate excretion in the kidneys, and reduction of circulating calcitriol concentrations in response to high phosphate (Fukagawa, Nii-Kono, & Kazama, 2005). The physiological action of FGF23 signaling in renal cells is suggested to function as follows: FGF23 binds

to FGF receptors (FGFR), with a protein termed Klotho serving as essential cofactor to enhance its affinity to the FGFR (Urakawa et al., 2006). Activation of the receptor leads to inhibition of renal phosphate reabsorption by reduction of renal mRNA and protein levels for the type IIa sodium-phosphate cotransporter (NaPi-2a) in the proximal tubular epithelium (Shimada et al., 2004). In chronic kidney disease (CKD), circulating FGF23 was shown to rise dramatically with a decline in renal function (Wolf, 2012). Recent studies suggest that a deficiency of Klotho represents one of the pathological mechanisms in chronic renal disorders (Olauson & Larsson, 2013), eventually leading to a switch in FGF23 induced signaling in cells with a lack of Klotho, but instead with the fibroblast growth factor receptor 4 (FGFR4) present. Klotho-independent activation of FGFR4 has been shown to lead to hypertrophy and fibrosis in cardiac myocytes (Grabner et al., 2015, pp. 3-5).

1.9 Rationale of this study

Since tissue sodium concentrations were shown to correlate *in vivo* with glycosaminoglycan content, and the steady state expression of XYLT1 mRNA encoding the enzyme that initiates GAG synthesis concentrations, the goal of this study was to investigate the potential regulation of XYLT1 expression, in the context of sodium biology, in order to gain further insight into regulatory mechanisms of tissue sodium storage. For this purpose, an *in vitro* cell culture system with pathway specific reporter constructs was to be established, to serve as a tool for internal control of successful stimulation of their respective intracellular pathways independently of the resulting effect on XYLT1 expression. K4IM cells, SV40 large T antigen immortalized human dermal fibroblasts, were used as a model for tissue fibroblasts and HEK 293 cells were used as model for parenchymal renal cells. We sought to determine if XYLT1 expression would be actively modulated in our *in vitro* systems by treatment with the following external stimuli:

1) Hyperosmotic environment. Intuitively, high extracellular sodium concentrations could be thought to stimulate non-osmotic sodium storage as a compensation mechanism. XYLT1 was also shown to correlate with calculated osmolality *in vivo*.
2) Vasopressin, as its main role is to maintain the stability of the body fluid osmolality and is increased with raising osmolality.
3) Endothelin 1 is shown to be involved in Na^+ homeostasis during conditions of elevated salt intake.
4) FGF23 functions as an important mediator in phosphate homeostasis via sodium-dependent phosphate transport and is known to increase under decreasing kidney function.
5) TGF-β, as amongst its numerous functions, it has been suggested to influence GAG synthesis and is known to play a role in progression of kidney disease.

2 Material and methods

2.1 Material

2.1.1 Cell culture

2.1.1.1 Cells

Table 1: Cells

Cell line	Medium	Origin
K4IM cells, human fibroblast cell line immortalized with SV40 T Antigen	DMEM with 10% FCS and 1% PS	The cell line was a gift from Prof. Haas, Freiburg (Germany)
HEK293 cells, adherent human embryonic kidney cell line	DMEM with 10% FCS and 1% PS	ATCC CRL-1573 Manassas, Virginia (USA)

2.1.1.2 Media and supplements

Table 2: Cell culture media and supplements

Name	Manufacturer
Blasticidin S HChl, 10 mg/ml	Life technologies™, Carlsbad (USA)
Dimethyl sulfoxide (DMSO)	Merck, Darmstadt (Germany)
Dulbecco's Modified Eagle's Medium (DMEM)	Life technologies™, Carlsbad (USA)
Dulbecco's Phosphate Buffered Saline (DPBS)	Pan Biotech GmbH, Aidenbach (Germany)
Fetal calf serum (FCS)	Biochrom GmbH, Berlin (Germany)
Penicillin/Streptomycin (P/S)	Biochrom GmbH, Berlin (Germany)
Trypsin/EDTA	Pan-Biotech GmbH, Aidenbach (Germany)
Trypan Blue 0.4% Solution	Lonza AG, Basel (Switzerland)

2.1.2 Bacteria

One Shot® Mach1™ T1 Phage-Resistant Chemically Competent E. coli, Invitrogen™, Carlsbad (USA).

2.1.3 Buffers and solutions

2.1.3.1 Molecular biology

Table 3: Buffers and solutions molecular biology

Name	Manufacturer
1kb DNA ladder	Thermo Fisher Scientific, Waltham (USA)
Basic Nucleofector Solution for Mammalian Fibroblasts	Lonza AG, Basel (Switzerland)
Buffers for DNA restriction enzymes	NEB, Ipswich (USA)
Buffer TE, endotoxin-free	Quiagen, Hilden (Germany)
dATP	Fermentas™, Waltham (USA)
dCTP	Fermentas™, Waltham (USA)
dGTP	Fermentas™, Waltham (USA)
dTTP	Fermentas™, Waltham (USA)
Loading buffer for agarose gels:	
0.25% Bromphenol blue	Roth, Karlsruhe (Germany)
0.25% Xylen Cyanol FF	Merck, Darmstadt (Germany)
30% Glycerol	Roth, Karlsruhe (Germany)
T4 DNA ligase buffer	Neb, Ipswich (USA)
Tris-borate-EDTA (TBE) buffer solution:	
90 mM Tris	Roth, Karlsruhe (Germany)
2mM borid acid 0.01M	Merck, Darmstadt (Germany)
EDTA, ph 8.0	Roth, Karlsruhe (Germany)

2.1.3.2 qPCR

Table 4: Buffers and solutions qPCR

Name	Manufacturer
Acrylamid	Amnion Biosciences, Bangalore (India)
DTT	Invitrogen™, Carlsbad (USA)
dNTP Set	Fermentas™, Waltham (USA)
First strand buffer	Invitrogen™, Carlsbad (USA)
Hexanucleotide Mix, 10 x conc.	Roche AG, Basel (Switzerland)
SYBR green master mix per 500µl:	
100µl 10x Taq Buffer	Fermentas™, Waltham (USA)
7.5 µ dNTP 25 mM	Fermentas™, Waltham (USA)
20 µl Rox reference dye	Invitrogen™, Carlsbad (USA)
200 µl PCR Optimizer LC120-0001 1ml	Bitop, Witten (Germany)
10 µl BSA PCR grade	Fermentas™, Waltham (USA)
2 µl SYBR green I 1:100, in 20% DMSO-H20	Sigma Aldrich, St. Louis (USA)
120 µl $MgCl_2$ 25mM	Fermentas™, Waltham (USA)
40.5 µl Aqua ad injectabilia	Braun, Melsungen (Germany)

2.1.3.3 Microbiology media and solutions

Table 5: Microbiology media and solutions

Name	Content
Ampicillin Stock solution	50 mg/ml Ampicillin, 70% Ethanol, 30% H20
LB medium per liter	10 g Bacto Tryptone, 10 g NaCl, Yeast Extract
LB Agar plates per liter	15 g Bacto Agar, 5g Bacto Yeast Extract, 10 NaCl, 10 g Bacto Tryptone
SOC medium	20 g Bacto Tryptone, 2.5 mM KCL, 5 g Yeast Extract, 10mM NaCl, 10 mM MgCl, 10 mM $MgSO_4$, 20 mM Glucose

2.1.4 Chemicals

Table 6: Chemicals

Name	Manufacturer
Agarose ultrapure	Thermo Fisher Scientific, Waltham (USA)

Aqua ad injectabilia	Braun, Melsungen (Germany)
β- Mercaptoethanol	Roth, Karlsruhe (Germany)
Ethanol, absolute	Merck, Darmstadt (Germany)
Ethidiumbromid 1%	Merck, Darmstadt (Germany)
Sodium chloride	Sigma Aldrich, Taufkirchen (Germany)
RNAse free water	Invitrogen™, Carlsbad (USA)

2.1.5 Enzymes

Table 7: Enzymes

Enzyme	Manufacturer
Antarctic Phosphatase	NEB, Ipswich (USA)
DNAse I	Quiagen, Hilden (Germany)
Phusion DNA Polymerase	NEB, Ipswich (USA)
Restriction enzymes	NEB, Ipswich (USA)
SuperScript II Reverse Transcriptase	Invitrogen™, Carlsbad (USA)
T4 DNA Ligase	NEB, Ipswich (USA)
Taq DNA-Polymerase	NEB Ipswich (USA)

2.1.6 Recombinant proteins

Table 8: Recombinant proteins

Name	Manufacturer
[Arg^8]Vasopressin acetate salt	Sigma-Aldrich, Saint Louis (USA)
FGF-23 human, recombinant, expressed in E.Coli	Sigma-Aldrich, Saint Louis (USA)
TGFβ-1, recombinant, source HEK293 cells	Acris Antibodies, Inc, San Diego (USA)
TGFβ-3, recombinant, expressed in E.coli	Sigma-Aldrich, Saint Louis (USA)
Endothelin-1 (human, porcine)	Tocris, Bioscience, Bristol (England)

2.1.7 Primer sequences qPCR

Table 9: Primer qPCR

Primer	Sequence 5'-3'	Characteristics	Manufacturer
18s_FW	GCAATTATTCCCCATGAACG	20 bp, Tm 55°C	Metabion international AG, Martinsried (Germany)
18s_RV	AGGGCCTCACTAAACCATCC	20 bp, Tm 59°C	
CHSY1_FW	TGTACACCACCCATGAGGAC	20 bp, Tm 61.5 °C,	Invitrogen™ Custom Primers, Carlsbad (USA)
CHSY1_RV	ACCCCTTTTTGTTCTGCTCG	20 bp, Tm 59.2 °C, cDNA specific	
CHPF2_FW	GACGCTGCCTCATTGACTCT	20 bp, Tm 62.8°C,	Invitrogen™ Custom Primers, Carlsbad (USA)
CHPF2_RV	CCCTATTTTTGGCCAGTTCA	20 bp, Tm 60.5 °C, not cDNA specific	
TGFB_FW	CAGCACGTGGAGCTGTACC	19 bp, Tm 62°C	Metabion international AG, Martinried (Germany)
TGFB_RV	AAGATAACCACTCTGGCGAGTC	22 bp Tm 62°C	
XYLT1_FW	CTCTGGATCCACACCCAAGT	20 bp, Tm 59.1 °C,	Invitrogen™ Custom Primers, Carlsbad (USA)
XYLT1_ RV	TTGCTGTCTGTTCGCACTTT	20 bp, Tm 58.6 °C, cDNA specific	

2.1.8 Plasmids

Table 10: Plasmids

Plasmid	Source
pcDNA-Gluc3-CMVMin	C. Jäckel
pCMV (CAT) T7- SB100	The plasmid was a gift from Zsuzsanna Izsvak (Addgen plasmid #34879)

2.1.9 Kit systems

Table 11: Kit systems

Name	Manufacturer
BioLux Gaussia Luciferase Assay Kit	NEB, Ipswich (USA)
Endofree Plasmid Maxi Kit	Quiagen, Hilden (Germany)
Innuprep Plasmid Mini Kit	Analytik, Jena (Germany)
Pure Link RNA Mini Kit	Invitrogen™, Carlsbad (USA)
QIAquick Gel extraction Kit	Quiagen, Hilden (Germany)

2.1.10 Consumables

Table 12: Consumables

Name	Manufacturer
Cell culture flasks	TPP, Trasadingen (Switzerland)
Cell culture plates	TPP, Trasadingen (Switzerland)
Centrifuge tubes 15 ml	BD Biosciences, Franklin Lankes (USA)
Cryotubes	Alpha Laboratories, Eastleigh (England)
Tubes, 5 ml 75x12mm, PS (Luminometer)	Sarstedt, Nürnbrecht (Germany)
qPCR multiwell plates	Sarstedt, Nürnbrecht (Germany)

2.1.11 Equipment

Table 13: Equipment

Name	Manufacturer
CO^2 incubator New Brunswick™ Galaxy® 48	Eppendorf, Hamburg (Germany)
LightCycler® 480 Instrument	Roche AG, Basel (Switzerland)
Microscope	Leika microsystems, Wetzlar (Germany)
Nano Drop ND-1000 Spectrophotometer	PEQLAB Biotechnologie GmbH, Erlangen (Germany)
Nucleofector™ 2b Device	Lonza AG, Basel (Switzerland)

PCR machine Mastercycler pro	Eppendorf, Hamburg (Germany)
Photometer Lumat 9507	Berthold, Bad Wildbad (Germany)
Thermoblock, Thermomix comfort	Eppendorf AG, Hamburg (Germany)

2.1.12 Software

Table 14: Software

Name	Manufacturer
Clone Manager Professional 9.2	Sci-Ed, Denver (USA)
GraphPad Prism 7	GraphPad Software Inc. San Diego (USA)
Lightcycler ® 480 software, 1.5.0.39	Roche AG, Basel (Switzerland)

2.2 Methods

2.2.1 Cell culture

2.2.1.1 General cell culture

The K4IM cells and HEK293 cells were incubated at 37°C and 5% CO_2 in a suitable vessel with DMEM medium with 10% Fetal calf serum (FCS) and 1% Penicillin/Streptomycin (PS). To prevent contamination, all cell culture work was performed in a laminar flow hood. All reagents were warmed to 37°C in a water bath before use. Furthermore, for subculturing, the medium was removed and adherent cells were washed with Dulbecco's Phosphate Buffered Saline (DPBS) and detached with Trypsin-EDTA solution. When the detachment of the cells was visible under microscope, an equal volume of medium containing 10% FCS was added to stop the reaction. Subsequently, the cells were pelleted by centrifugation at 220 xg (rt) for 3 minutes. After resuspending the cell pellet in fresh medium, a fraction of the culture medium according to the desired split factor was seeded into a new cell culture flask and fresh medium was added.

2.2.1.2 Counting cells

Cells/ml were counted by using a Neubauer chamber. A sample was prepared by mixing an aliquot of the cell suspension 1:2-1:5 (depending on celldensity) with trypan blue solution (0.4%) to differentiate viable from dead cells. Subsequently, 10 µl of the mixture was pipetted into the counting chamber. Under the microscope, the living cells were counted in all four quadrants of the chamber. The number of cells/ml was calculated as follows:

$$\frac{Count\ of\ cells}{number\ of\ quadrants} * the\ dilution\ factor * 10^4 = number\ of\ cells/ml$$

2.2.1.3 Freezing and thawing cells

Cells were frozen in cryotubes to minimize genetic change and avoid contamination. Freezing medium contained the respective culture medium of the cells +10% Dimethyl sulfoxide (DMSO). The tubes were stored at -80°C freezer over 24h prior to transferring them into a tank with liquid nitrogen for long time storage. The frozen cells were thawed in a 37°C water bath and rapidly transferred into a cell culture flask with prewarmed medium to dilute DMSO to non-toxic concentration. After 24h, the medium was exchanged to remove DMSO completely.

2.2.2 Molecular biology

2.2.2.1 Polymerase chain reaction (PCR)

PCR is a method to amplify a selected DNA sequence using a heat-stable DNA polymerase. A repetitive amplification allows the synthesis of millions of copies in short time. In each cycle, the amount of the selected DNA doubles, which leads to an exponential increase. Nucleotide sequences of the flanking region of the target DNA were used to select suitable primers. The primers were provided by Invitrogen LifeTechnologies.

Per tube (25 µl), the following standard mix was prepared: 5x Reaction buffer (1:5), template DNA (500 ng), fw primer (400 nM), rv primer (400 nM), dNTPs (200 nM), Polymerase (4.5 units), H_20 (up to 225 µl). All polymerase chain reactions were performed after the following protocol:

Table 15: General PCR protocol

Step	Settings	Cycle count
Initial denaturation	98°C, for 3 min.	1
Denaturation	98°C, for 30 sec	30
Annealing of primers and DNA	Temperature depends on the primer, for 30 sec	30
Chain extension	72°C, time depends on size of the product	30
Final extension	72°C for 10 min	1
Final hold	10°C	1

After separation of the double stranded target DNA into single strands, so called denaturation, the separated strands were cooled for annealing of the primers. The annealing temperature was set up individually for each PCR, depending on the primers. In the next step, complementary copies of the target were produced by the DNA polymerase. After completion of one cycle of replication, the reaction mixture was heated up again. After binding of each DNA strand to a complementary primer, the cycle of chain extension was repeated. In total, 30 cycles were performed before final extension.

After completion of the PCR, agarose gel electrophoresis was used for analysis and purification of the resulting products.

2.2.2.2 Agarose gel electrophoresis

Agarose gel electrophoresis is a common method to separate DNA fragments or proteins using agarose as a matrix. The DNA fragments were separated and DNA was visualized using ethidium bromide, a DNA intercalating agent that fluoresces under UV light. The percentage of agarose in the agarose gel was chosen after the expected size of the DNA fragments; 2% for smaller fragments consisting of <800 base pairs (bp) and 0.6% for larger fragments consisting of >1000 bp. For preparation of the gel, the agarose powder was dissolved in Tris-borate-EDTA (TBE) buffer with added ethidium bromide, and heated to near-boiling point in a microwave before it was casted in the gel chambers. Loading buffer for agarose gels (6x) was mixed with the DNA samples and a size standard. Subsequently, the mixture was pipetted into the wells. During the electrophoresis, which was performed at 120 V, the gel was completely submerged in TBE buffer. Then, the DNA was visualized under UV light and the gels were photographed for documentation. In case of further use of the separated DNA fragments, the DNA bands were cut out of the gel under UV light. For subsequent DNA extraction from the gel, Qiagen gel Extraction Kit was used according to the manufacturer's instructions.

2.2.2.3 Sequencing of DNA

For sequencing, the samples were sent to GATC Biotech company.

2.2.2.4 Measurement of DNA concentration

A nanodrop spectrophotometer was used, according to the manufacturer's instructions to measure the amount of DNA in a solution. After initializing the nanodrop with 2 µl RNase free water, the measurements were made from 2 µl of each sample.

2.2.2.5 DNA restriction digestion

To identify suitable restriction enzymes to cut the plasmids within a specific restriction site, CloneManager Software was used. For the digestion mix, the following rule was respected: For

digestion of 1 µg DNA, 1 unit of enzyme was added per hour, up to a maximum of 10% of the total volume. The buffer found to be most compatible with the enzymes was used according to the suggestion of the manufacturer. Typical protocol (mixed in a microfuge tube): 1 µl 10x buffer, 5.7 µl H_20, 3µl DNA (100ng/µl), 0.3 µl enzyme. After brief vortexing and centrifugation, the mixture was incubated for 1h at a suitable temperature (37°C-65°C).

2.2.2.6 End modification: Dephosphorylation

In order to prevent re-ligation of vectors, the 5'phosphate group was removed after digesting DNA with the Antarctic phosphatase according to the manufacturer's instructions. It was then purified using a commercially available kit.

2.2.2.7 Ligation of DNA fragments

To insert the DNA of interest into a vector backbone, T4 DNA ligase enzyme was used according to the manufacturer's instructions. Molar ratio 1:3 vector to insert. T4 DNA ligase was added last. 20µl reaction: 2µl T4 DNA ligase buffer 10x, vector DNA (4kb) 50 ng, insert DNA (1 kb) 37.5 ng, T4 DNA Ligase 1 µl. Nuclease-free water to 20 µl.

2.2.2.8 Transformation of competent E. coli Mach 1

The process of transformation was used to introduce the plasmid of interest into chemically competent E. coli bacteria. The bacteria carrying the plasmid were grown up and selected by antibiotics. For the transformation, frozen E. coli Mach-1 bacteria stored at -80°C were rapidly thawed on ice. 10-100 ng of DNA was added to 50µl of the bacteria suspension in a tube. After mixing gently, the mixture was incubated for 5 to 30 min on ice and subsequently heat shocked at 42°C for 45 seconds before transferring it back on ice for cooling. 250 µl SOC medium was added, followed by a 60 min incubation at 37°C and 500 rpm. Then, the mixture was plated onto pre-warmed agar plates with an appropriate selective antibiotic for subsequent incubation over night at 37° C. Concentration of selective antibiotics: Kanamycin 50 µg/ml, Ampicillin 120 µg/ml.

2.2.2.9 Isolation and analysis of plasmid DNA from transformed E. coli bacteria

Single colonies from the agar plates or the backup plate were transferred into liquid cultures (LB-medium containing the selection antibiotic). The liquid cultures were then incubated overnight on a warmed shaking device (300 rpm). Commercially available kits were used for isolation according to the manufacturer's instructions (*Innuprep Plasmid Mini kit* for liquid culture up to 5 ml, *Quiagen Endofree plasmid max kit* for liquid cultures up to 100 ml). The plasmid DNA extracted by minipreparation was used to analyze the clones. The DNA was digested using appropriate

restriction enzymes and the resulting fragments were then analyzed by agarose gel electrophoresis. Maxipreparation was performed to gain up to 300-500 µg of purified DNA for further use. DNA-concentration was measured using the nanodrop photometer (see 2.2.2.4).

2.2.3 Cloning strategies

The tools present in our laboratory were used. Cloning of the vectors was mainly conducted by Carsten Jäckel and Nadja Ehni.

2.2.3.1 Traditional cloning strategy

The plasmids were cloned using traditional cloning. Restriction enzyme cloning and T4 DNA Ligase were used for the modification steps in the vectors backbones described in 2.2.3.2. according to the manufacturer's instructions (Jackel et al., 2016, p. 2).

2.2.3.2 Design of pcDNA-Gluc3-Promotor vector

To monitor the activation status of regulatory pathways, a reporter vector system was designed in our laboratory by Carsten Jäckel (Jackel et al., 2016). For this purpose, the commercially available pcDNA6/TR TET Repressor expression vector (Thermo Fisher Scientific, Walham, USA) was modified in multiple ways (Jackel et al., 2016, p. 2). First, inverted terminal repeats compatible for SB100 transposase (SB ITRs) were introduced, allowing stable integration of transgenes into cell genomes by an active mechanism (Jackel et al., 2016, p. 2). Then, a modified Gaussia Luciferase reporter cassette based on the commercially available pGL3-Promoter Vector (Promega, Fitchburg, USA) was inserted, that contains *Gaussia princeps* instead of Firefly luciferase and a cytomegalovirus promoter replacing the SV40 minimal promoter for less background activity (Jackel et al., 2016, p. 2). The function of the TET-Repressor was retained. The resulting vector, which in this work is named pcDNA-GLuc3-CMVMin Vector, was published by Jackel et al. (2016) under the name pSBTET.reporter.

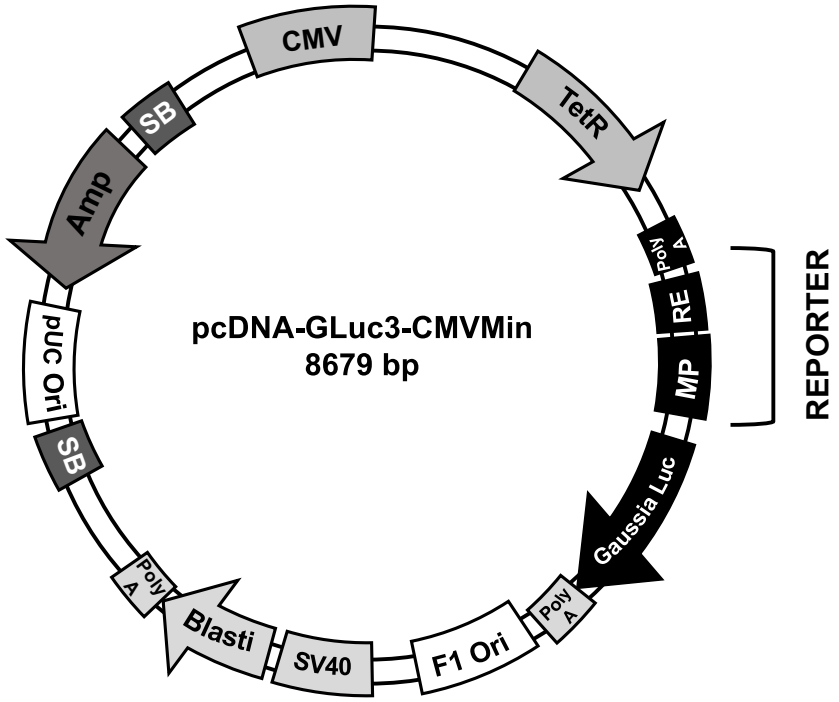

Figure 6: pcDNA-GLuc3-CMVMin

SB= Sleeping beauty transposon inverted terminal/direct repeats. CMV= Cytomegalovirus Promoter, TetR: TetRepressor. Poly A= polyadenylation signal sequence. MP= minimal promoter. RE= transcription responsive elements. Gaussia Luc= CDS of the Gaussia luciferase. F1 ori= origin of replication. SV40= SV40 Promoter. Blasti= Blasticidin resistance gene. Amp= Ampicillin resistance gene for bacterial selection.

2.2.3.2.1 Sleeping Beauty transposon system

Delivery of DNA molecules into mammalian cells is often inefficient and the expression of the transgene is brief due to intracellular breakdown. To optimize the potential for the generation of stable transfectants, Sleeping beauty (SB) transposon system was used. It is a non-viral vector system allowing for the efficient stable integration of transgenes into genomes by an active mechanism. The gene of interest is flanked by SB-transposon inverted terminal repeats (ITR). The SB transposase compatible reporter is cotransfected into cells with a plasmid carrying the transposase enzyme gene. The SB transposase can so bind to the ITR and cuts the transposon out of the plasmid to insert it into a new DNA locus.

2.2.3.2.2 Gaussia Luciferase reporter protein

The pcDNA-GLuc3-CMVMin Vector uses Gaussia Luciferase (GLuc) as reporter protein, a naturally secreted protein by the *copepod, Gaussia princeps*, that catalyses the oxidation of the substrate coelenterazine in a reaction that emits light. The amount of light can be measured directly from the supernatant of the cells without cell lysis. To perform luciferase reporter assays of a gene of interest, the transcription factor responsive elements (RE) associated to that gene have to be introduced into the vector's backbone. These responsive elements function then together with a minimal promoter element to modulate the activity of the luciferase reporter gene.

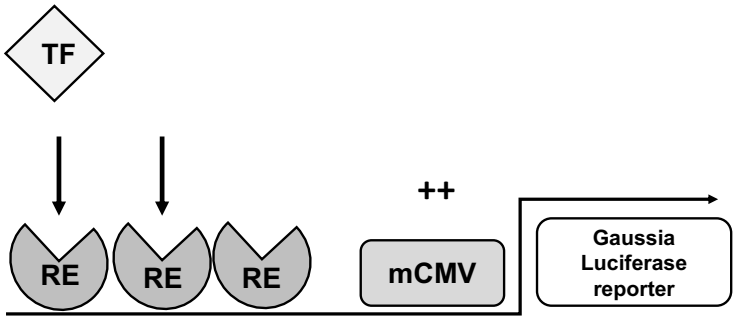

Figure 7: Modulation of the Gaussia luciferase reporter activity

The transcription factor binds to the transcription-response-element whereby the Cytomegalovirus-promoter activity gets enhanced, subsequently leading to increased Luciferase activity. The produced luminescence can be measured in the supernatant of the cells. It increases proportional to the amount of enzyme, which in turn, reflects the level of transcription. TF= transcription factor, RE= transcription-response-element, mCMV= minimal Cytomegalovirus-promoter.

2.2.3.3 Introduction of responsive elements into pcDNA-Gluc3-CMVMin Vector

For the generation of specific reporter vectors, designed multimers of bindings sites for pathway-associated transcription factors were ligated into the pcDNA-Gluc3-Promotor vector backbone by Pstl and Xhol digests (Jackel et al., 2016, p. 2).

2.2.3.3.1 TGF-β/SMAD reporter

This TGF-β/SMAD reporter is a reporter for TGF-β/SMAD-based signaling. The amount of TGF-β dependent reporter expression in the stably transfected cells can be measured by assaying the Gaussia Luciferase activity that is secreted into the growth media. A series of SMAD consensus

binding elements are located in front of a minimal CMV promoter. The system consists of eleven SMAD binding elements (5x multimer): AGCCAGACAGT. It was ordered synthetically and then ligated between the Xhol and Pst I sites of the pcDNA-Gluc-CMVMin backbone (Jackel et al., 2016). The resulting vector is here named pcDNA-Gluc3-CMVMin-TGFv2.

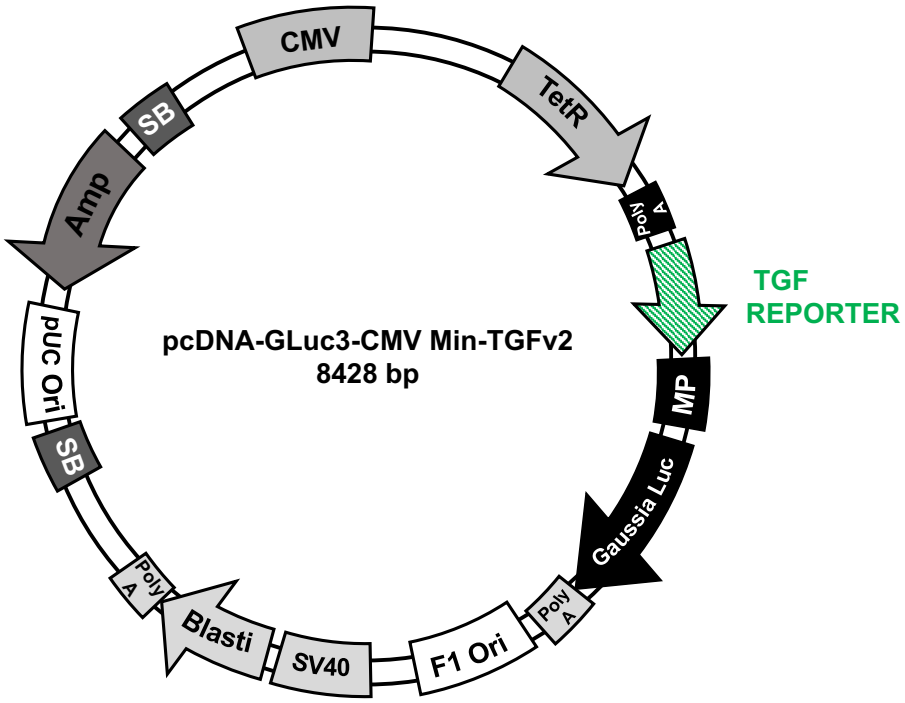

Figure 8: TGF-β/SMAD reporter

The SMAD element was ligated into the backbone of the pcDNA-Gluc-CMVMin-Vector.

2.2.3.3.2 NFAT5 reporter

The NFAT5 reporter is a reporter for activation of the NFAT5 signaling pathway, that is involved in the activation of a response to hyperosmotic stress. A series of NFAT5 binding elements are located in front of a minimal CMV promoter. The reporter consists of the dimer CAGCGG-TAATTTTCCACCA, synthetically produced and ordered from a manufacturer for this purpose. The binding element was ligated between the Xhol and Pst I sites of the pcDNA-Gluc-CMVMin backbone (Jackel et al., 2016). The resulting vector is here named pcDNA-Gluc3-CMVMin-NFAT5.

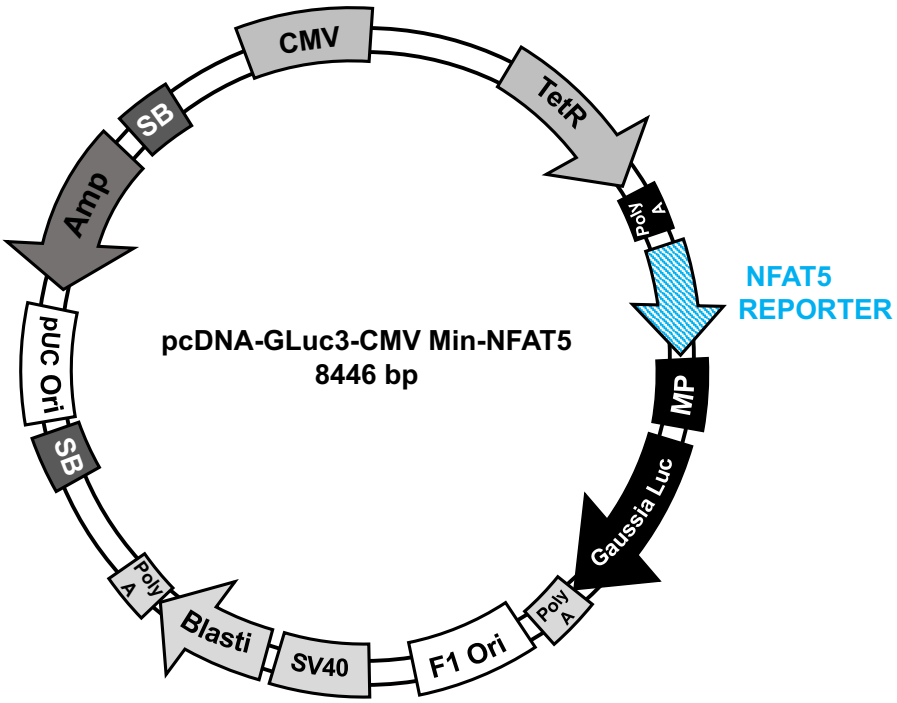

Figure 9: NFAT5 reporter

The NFAT5 element was ligated into the backbone of the pcDNA-Gluc-CMVMin-Vector.

2.2.4 *In vitro* experiments

2.2.4.1 Stable transfection of cells using nucleofection and Sleeping Beauty transposase

Transfection describes the process of adding foreign DNA into eukaryotic cells. There exist various transfection methods. Here, nucleofector technology (Lonza, Basel, Switzerland) was used to transfect plasmid DNA into the human dermal fibroblast cell line K4IM. This technology is based on electroporation and uses cell-type specific Nucleofector solution. By a device called Nucleofector, an electric pulse is generated and leads to an increase of the cell membrane permeability. This allows the foreign DNA in the medium to enter the nucleus of the cells.

For stable integration, reporter plasmids were cotransfected with pCMV (CAT) T7 SB 100 transposase expression plasmid (see 2.2.3.2.1).

The fibroblast cell culture and the transfection procedure were performed according to the Amaxa Nucleofector protocol for Primary Mammalian Fibroblasts, as follows: Cells were subcultured 2-

4 days before nucleofection. When 70-90% confluent, the cells were detached and counted; the amount of $1*10^6$ cells per nucleofection sample was needed. After transferring the cells into a 1.5 ml centrifuge tube, the tube was centrifuged at 7000 xg for 1 min and the cell pellet was resuspended carefully in 100 µl room temperature Nucleofector Solution per sample. 100 µl of the cell suspension was then combined with 0.5 µg of the desired plasmid DNA and 1.5 µg pCMV(CAT)T7 SB 100. Subsequently, the cell/DNA suspension was transferred into a certified cuvette, avoiding air bubbles, and closed with a cap. After inserting the cuvette into the Nucleofector device, the nucleofection was performed using the 3T3 L1 pre ad (ATCCC) Nucleofector program. The cuvette suspension was then carefully transferred into a 25 cm^2 flask with 5 ml medium. After incubation at 37°C for 24 hours, the medium was removed and medium containing the selective antibiotic was added to start selection.

For transfection of the plasmids into Hek293 cells, the transfection procedure was performed according to the Amaxa Nucleofector protocol provided for HEK-293.

Table 16: Generation of reporter cell lines

Cell line	Reporter construct	Resulting reporter cell line
K4IM cell line	pcDNA-Gluc3-CMVMin-TGFv2	TGF-β/SMAD reporter K4IM cells
	pcDNA-Gluc3-CMVMin-NFAT5	NFAT5 reporter K4IM cells
Hek293 cell line	pcDNA-Gluc3-CMVMin-TGFv2	TGF-β/SMAD reporter HEK293 cells

2.2.4.2 Selection of the transformants

Stably transfected cells were selected using the antibiotic blasticidin, based on the selective marker present in the vector backbone. The lethal dose, depending on the cell line, was determined by an individual experiment using a dilution row. The lowest concentration found to kill all non-transfected cells within 10 days, 0.8 µl of 10 mg/ml Blasticidin per 1 ml medium, was then used to select for stable transformants.

2.2.4.3 Validation of signal pathways stimulation of specific reporter cell lines

The reporter cell lines were detached, counted and seeded in triplicate per treatment group into 12-well format, 60 000 cells per well, in 1 ml DMEM medium/well without additives. As a control, cells without reporter construct were seeded. After 24 hours of incubation, stimulation was performed. 24, 48, and 72 hours after stimulation, reporter activity was assessed by sampling

supernatants for luciferase activation. Then, the cells were lysed, and RNA isolation, reverse transcription and RT-PCR were performed as described in 2.2.5.

2.2.4.4 Gaussia Luciferase Assays

The reporter constructs use Gaussia Luciferase as a reporter protein (see 2.2.3.2.2). After addition of its substrate Coelenterazine to the cell culture supernatant, the measurement of the amount of light in relative light units (RLU) produced in this reaction was carried out using a luminometer. The commercially available BioLux Gaussia Luciferase Flex Assay Kit was used according to the manufacturer's instructions. To prepare the Gluc assay solution, 50 µl assay puffer, 0.5 µl substrate and 8 µl stabilizer per sample were mixed. After incubating at room temperature for 25 minutes protected from light, 50µl of the prepared solution was added to 20 µl of cell culture supernatant in 5 ml tubes. After incubation of minimum 45 seconds, the luminescence was measured using a Berthold Lumat LB 9507 Luminometer with 10 seconds measurement. As a control, 50 µl of pure Gluc assay solution without supernatant was measured and subtracted from the result of the samples.

2.2.5 Quantitative real-time PCR

Total RNA was isolated from the cells and reverse-transcribed to complementary DNA (cDNA). Then, qPCR was performed to quantify the resulting cDNA in real time and so determine the relative amount of mRNA for a specific gene.

2.2.5.1 Total RNA purification

To isolate RNA from the cells used in the cell-culture experiments, PureLink RNA Mini Kit (Thermo Fisher, Waltham, USA) was used according to the manufacturer's instructions. To remove residual DNA from the sample, the optional digestion step with DNase I (Qiagen, Hilden, Germany) was included. In brief, the adherent cells were disassociated from the vessel using Trypsin and pelleted by centrifugation. Then, the cells were lysed with 600 µl lysis buffer containing 1% 2-mercaptoethanol, the solution was homogenized by vortexing. Subsequently, the same volume of 96-100% ethanol was added to the sample and mixed thoroughly by vortexing. The sample was then processed through a spin cartridge with a collection tube to bind RNA to a membrane. After Centrifugation (12.000 xg for 15 seconds), the flow-through was discarded. 350 µl wash buffer I was added to the spin cartridge. After centrifugation (12.000 xg for 30 seconds), the flow through was discarded. Then, 80 µl purelink DNase mixture (In RNAse free water resuspended DNase mixed with RDD buffer 1:8) was added directly to the surface of the spin cartridge membrane. After 15 minutes incubation at room temperature, another 350 µl of wash buffer I was added to the spin cartridge and the flow-through was discarded once again after centrifugation (12.000 xg for 30 seconds) Subsequently, the spin cartridge was inserted into a new collection

tube followed by two rounds of washing with wash buffer II with ethanol, centrifugation and discard of the flow-through. Then, to dry the membrane with attached RNA, the spin cartridge was centrifuged at 12.000 xg for 1 minute and inserted into a recovery tube. 35 µl RNase-free water was added to the center of the spin cartridge. After incubation for 1 minute at room temperature, the spin cartridge and recovery tube were centrifuged at 12.000 xg for 2 minutes. Thereafter, the purified RNA of each sample was so eluted in 35 µl RNase-free water.

2.2.5.2 Reverse transcription

The RNA samples were then processed to cDNA through reverse transcription. For the reverse transcription, the total amount of purified RNA in a volume of 30 µl RNase free water was added to 15 µl of the RT+ reaction mix (RT+ sample).

A so called RT- control was added this reaction step to exclude PCR signal caused by contamination with genomic DNA. For the RT- sample, RNA in a volume of 3 µl RNase free water was diluted with 27 µl RNase free water (dilution factor 1:10) and then added to a reaction mix equal to the RT+ reaction mix with the exception of the reverse transcriptase enzyme.

Table 17: Reverse transcription, reaction mix

Reagent	**RT+**	**RT- (1:10)**
First-strand buffer (5x)	9.0 µl	9.0 µl
dNTP 25 mM	1.0 µl	1.0 µl
DTT 0,1 M	2.0 µl	2.0 µl
Rnasin 40 U/µl	1.0 µl	1.0µl
Acrylamid (linear) 15 µg/ml	0.5 µl	0.5 µl
Hexanucleotide 2µg/µl	0.5 µl	0.5µl
Superscript 200 U/µl	1.0 µl	-
H_2O RNasefree	-	1.0 µl
TOTAL	**15µl mix/sample**	**15 µl mix/sample**

After adding the reaction mixes to the RT+ and RT- samples, both were incubated at 42 °C in a thermoblock and shaken for 90 minutes (350rpm). Then, the samples were stored at -20 °C until needed for further use. Since no reverse transcription could take place in the RT- sample and RNA is not measurable in qPCR, any signal produced by RT- had to come from DNA contamination

or cDNA unspecific primer. For subsequent qPCR reaction, a 1:10 dilution of the RT+ samples was needed (5 µl of the RT+ samples was diluted with 45 µl RNase free water), while the RT- samples were already diluted before reverse transcription and did not need further dilution to reach equal amount of RNA in the RT+ and RT- reactions.

2.2.5.3 Quantitative PCR (qPCR)

Quantitative PCR monitors the amplification of a targeted DNA molecule during the PCR by detecting fluorescent signals. There exist multiple variants of qPCR. Here, the LightCycler® 480 instrument with the SYBR Green method was used. SYBR Green is an intercalating dye, which specifically binds all double-stranded DNA. It exhibits very little fluorescence in its unbound state in solution and fluoresces only in its DNA bound state (measured at 530 nm at the end of each elongation phase). The fluorescent signal measured by the qPCR cycler device increases during the PCR cycles, correlating with the amount of dsDNA generated. This allows for calculation of the number of input copies of the target nucleic acid. Relative abundance of the original mRNA in a sample will result in an earlier detection of fluorescent signal than for samples with lower amounts. However, SYBR green detects all double-stranded DNA unspecifically, including non-specific PCR products. To determine whether only the desired PCR product has been amplified, an additional step follows after the amplification cycles: A melting curve analysis is performed, based on the fact that each double-stranded DNA molecule has its characteristic melting temperature (T_m), depending on length and GC content. The melting of dsDNA leads to sharp decrease of SYBR Green I fluorescence (=loss of signal) when the temperature reaches the melting temperature of the PCR product. This is used as a control: If there was generated only one amplicon, a single peak appears in the melting curve analysis. The appearance of additional melting peaks indicates the presence of unspecific products or DNA contamination.

To analyze the data from qPCR, relative quantification was used. In this method, the expression of candidate genes is normalized to a reference gene, a so called housekeeping gene, which is a constitutively expressed gene in all cells. The expression should be as similar as possible under all experimental conditions. Here, the housekeeping gen S18 was used. The master mix for the qPCR reaction was prepared as follows, using SYBR Green master mix (including the fluorescent dye), qPCR primers and thermostable DNA polymerase. H_2O was added to reach a volume of 18 µl. Then the master mix was mixed by vortexing for 1-2 seconds and subsequent brief centrifugation.

Table 18: qPCR, reaction mix

Reagent	Amount per reaction per well
SYBRGreen mastermix	10 µl
SYBRGreen primer FW	0.6 µl (10 pM)
SYBRGreen primer RV 10 pM	0.6 µl (10 pM)
Taq Polymerase	0.12 µl (0.03 U/µl)
H_2O	6.68 µl
TOTAL	**18 µl**

96-Well PCR Plates were used as reaction plates; Experiments were set up in duplicates. All primers that were utilized are summarized in the table 9. First, 18 µl of the master mix was dispensed into each well of the reaction plate. Then, 2 µl of the RT+ (1:10) dilution or 2 µl of the RT- samples was added to the master mix to reach a final volume of 20 µl per well. As a negative control, 2µl water was added to the master mix instead of 2 µl from the samples. The multiwell plate was sealed with a thin sheet of plastic and was then briefly centrifuged. Subsequently, the plate was loaded into the LightCycler® 480 instrument; qPCR was performed, using the SYBR Green/HRM Dye protocol (excitation filter 465, emission filter 510), that exists of four steps: 1) *Pre-Incubation* for 5 minutes at 95 °C, which allows the activation of the Taq polymerase and the denaturation of the cDNA. 2) *Amplification* of the target DNA by cycling the samples 45 times at 95°C for 15-30 seconds and at 72°C for 5-30 seconds, causing denaturation and annealing/extension and measuring fluorescence. 3) *Melting curve* analysis to identify the PCR product. 4) *Cooling* of the plate with one cycle at 40°C.

2.2.5.4 Quantification analysis

During a PCR reaction, a certain amount of background fluorescence is seen. Therefore, an arbitrary threshold must be defined, representing a level above background fluorescence. During the amplification step in qPCR, this vertical threshold line is crossed by fluorescence in a certain cycle, so called crossing point-qPCR-cycle (C_p). The cycle where each reaction reaches the threshold depends on the amount of target DNA. Low C_p values indicate high amounts of target DNA, that rise above background in an early PCR cycle, whereas high C_p values indicate low amounts of target DNA, that rise above background in a late PCR cycle.

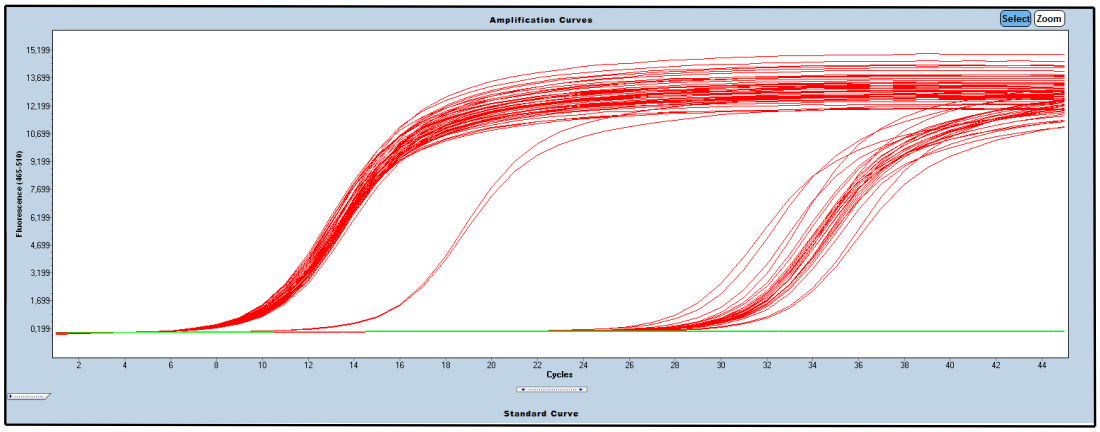

Figure 10: Amplification curves after performance of qPCR

The fluorescence emission proportional to the PCR product was visualized in amplification curves. Amplification curves are obtained using a dilution series of each sample. They consist typically of 3 phases, initiation phase, exponential phase and plateau.

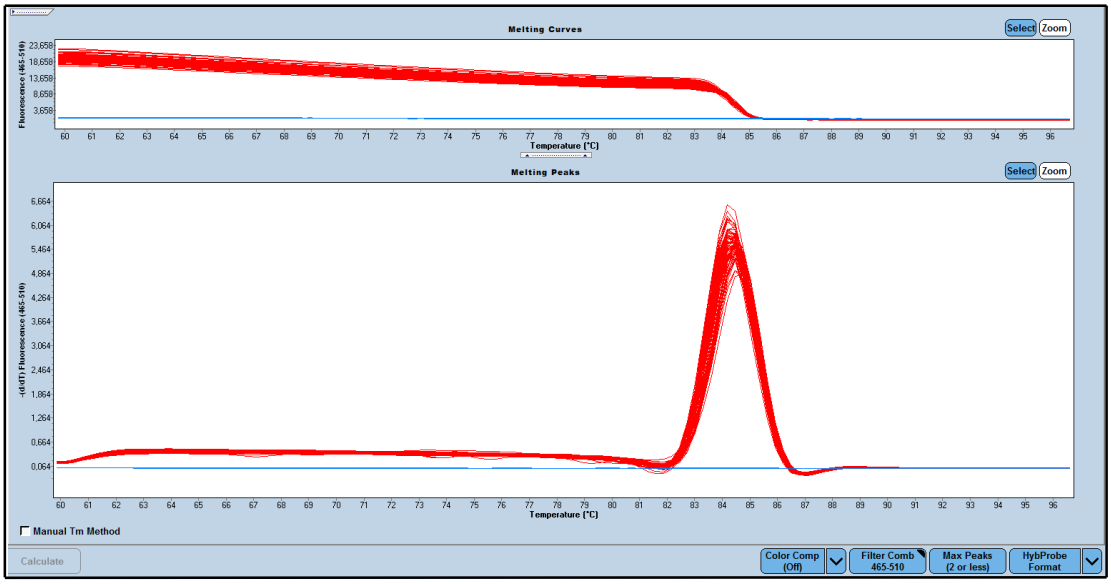

Figure 11: Melting curve analysis of the amplicons

Single peak. Unspecific products would be shown as additional peaks.

In relative quantification, a so called normalization to reference genes (housekeeper genes) was used. The target DNA template was compared with the reference gene in the same sample (Target/ref). That allowed comparisons across different samples. There exist different analysis modes for relative quantification. Here, advanced relative quantification analysis was performed using the LightCycler® 480 software, following the manufacturer's instructions. This analysis uses the so called efficiency method (E-method) that is based on standard curves, but takes into consideration the differences in target and reference-gene amplification efficiency when calculating the final result.

2.2.6 Statistical analysis

All stimulation experiments were conducted in triplicate to allow for assessment for significance. Data were analyzed by using GraphPad Prism software 5 (San Diego, CA, USA). Student's unpaired t-test was used for Gaussian distributed data. Statistical significance was identified in the graphs with p-values < 0.05 (*), < 0.01 (**) and < 0.001 (***) as determined by the software.

3 Results

For the *in vitro* cell culture system, the human dermal fibroblast cell line K4IM was selected as dermal fibroblasts are found in the connective tissue of the skin, where they produce procollagen and GAGs. The Hek-293 cell line, originally isolated from human embryonal kidneys, was chosen as model for kidney parenchymal cells. To study inducibility by TGF-β and salt respectively, reporter plasmids were first stably integrated into both cell lines. The activity of the respective pathway was then used as a tool for internal control of successful stimulation of their respective intracellular pathways, independent of the resulting effect on XYLT1 expression.

The Hek-293 cells carrying reporter plasmids did not display any XYLT1 inducibility (data not shown). Experiments performed under the same conditions, using reporter engineered K4IM cells, were more promising (see 3.2.). This led to the impression that the K4IM cell line was a better model system for studying XYLT1 induction rather than the Hek-293 cell line. As a result, only data from experiments carried out in transfected K4IM cells are included in the following sections.

3.1 Validation of the reporter vectors

After transfection of the individual reporter constructs into K4IM cells (see 2.2.4.1), the functionality of the reporter constructs was validated by stimulation of the individual pathway reporters. For each pathway, a stimulator for the pathway reporter was chosen: For the TGF-β/SMAD pathway, recombinant human TGF-β1 was used to activate the reporter construct (figure 12). For activation of the NFAT5 reporter, a hyperosmolar environment was created by stimulation with sodium chloride (figure 13). In order to determine a functional range of TGF-β1 and sodium chloride, and to study the dose dependent nature of the response, the stimulation was performed in a titration experiment.

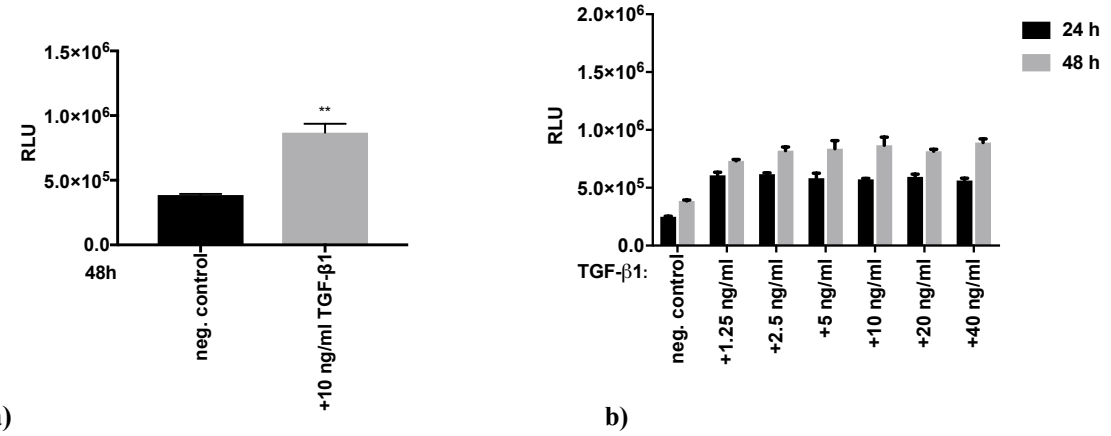

Figure 12: Validation of the TGF-β/SMAD reporter in TGF-β/SMAD reporter K4IM cells

a) Significant activation of the reporter construct by TGF-β1 b) Stimulation reaches a plateau with doses > 2.5 ng/ml. To assess activity of the TGF-β/SMAD reporter, stably transfected K4IM cells were treated with, or without, TGF-β1 in increasing concentrations for 24h and 48h, after which reporter activity was assessed by measuring luciferase activity in the supernatant. A 96-well plate with 10 000 cells per well, with three wells per treatment group was used. Data are represented as relative light units (RLU). As a control, unstimulated not transfected K4IM cells were incubated under same conditions and subtracted from the data. P= 0.0023. Statistical analysis was performed using the unpaired t-test to compare the two groups.

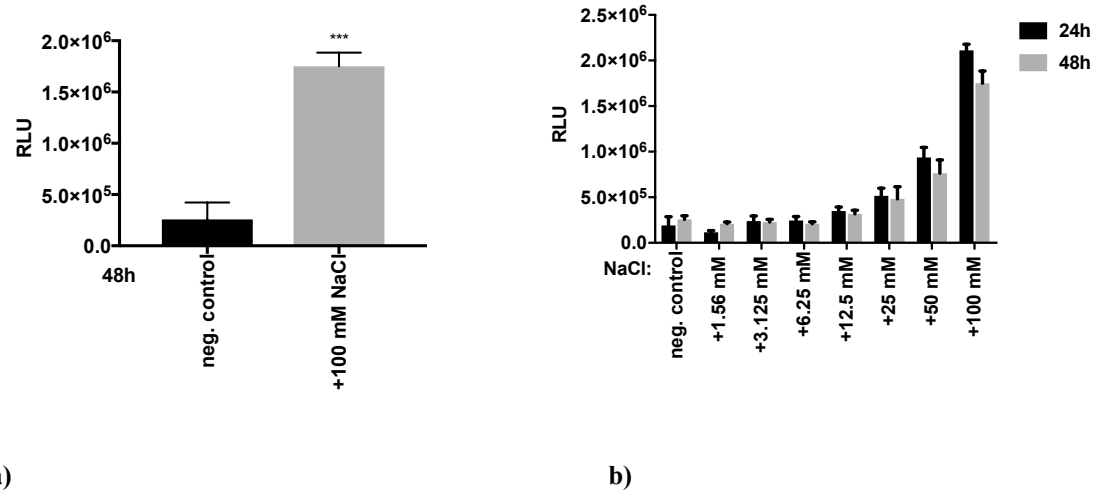

Figure 13: Validation of the NFAT5 reporter in NFAT5 reporter K4IM cells

a) Significant activation of the reporter construct by hypertonic sodium b) Dose dependent enhancement of reporter activity, with high NaCl doses (100 mM) found to be toxic to the cells. To assess activity of the NFAT5 reporter, stably transfected K4IM cells were treated with, or without, NaCl in varying doses for 24h and 48h, after which reporter activity was assessed by measuring luciferase activity in the supernatant. A 96-well plate with 10 000 cells per well, with three wells per treatment group was used. Molar concentrations of NaCl described here were added to the standard NaCl concentration in the growth medium. Data are represented as relative light units (RLU). As a control, unstimulated not transfected K4IM cells were incubated under same conditions and subtracted from the data. P<0.001. Statistical analysis was performed using the unpaired t-test to compare the two groups.

Stimulation of both constructs led to significantly increased Gaussia luciferase signal, verifying their functionality.

TGF-β1 concentrations above 2.5 ng/ml did not lead to a significant further increase of TGF-β/SMAD reporter activation, suggesting saturation of the reporter construct.

For the NFAT5 reporter, a dose-dependent enhancement of activation was shown, yielding the best stimulation results in sodium chloride concentrations between 50 mM and 100 mM. Toxic effects on the cells were observed at the highest concentration.

These results provided suitable concentration ranges of TGF-β1 and sodium chloride, to be used for more accurate measurements of reporter construct activation in the following experiments.

3.2 Stimulation experiments with TGF-β1

As XYLT1 expression was shown to be modulated by the multifunctional cytokine TGF-β in the *in vitro* model of Fischereder et al. (2017), an important objective in this study was to assess reproducibility of these findings in our reporter engineered K4IM cells. This was accomplished through a series of stimulation experiments. TGF-β/SMAD reporter cells were treated with or without recombinant human TGF-β1 for 24, 48 and 72 hours. Resulting relative XYLT1 expression was quantified using qPCR. Simultaneously, the TGF-β/SMAD reporter construct was used as a tool for internal control of successful stimulation.

A potent activation of the TGF-β/SMAD reporter was found, demonstrating successful stimulation. There was also found significant induction of XYLT1 mRNA expression relative to 18S RNA after one-time treatment with TGF-β1, after 24, 48 and 72 hours with TGF-β1 present in the growth media (figure 14).

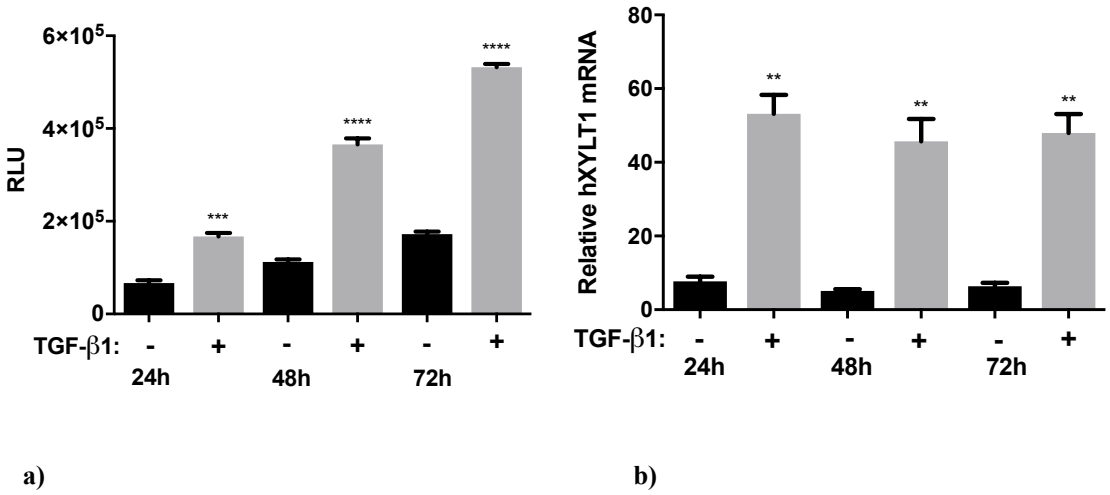

Figure 14: Treatment of TGF-β/SMAD reporter K4IM cells with recombinant TGF-β1

a): **TGF-β1 stimulation led to a clear activation of the reporter construct. Accumulation of the protein produced by luciferase in the supernatant led to increase of RLU values after 48h and 72h. b): Relative induction of XYLT1 expression by TGF-β1, equally strong 24h, 48h and 72h after stimulation.** K4IM cells with integrated TGF-β/SMAD reporter were grown to confluence in DMEM, without addition of FCS and penicillin/streptomycin. Next, the cells were stimulated one time with, or without, 10 ng/ml TGF-β1 and then incubated for 24h, 48h or 72h. Reporter activity was assessed by measuring luciferase activity in the supernatant. The data are represented as relative light units (RLU). After lysis of the cells, RNA isolation, reverse transcription and relative quantification by qPCR was performed. Data represent steady state levels of hXYLT1-mRNA normalized to S18 RNA. 12-well plates with 60 000 cells per well, with three wells per treatment group were used. As a control, unstimulated K4IM cells without integrated reporter were incubated under same conditions and subtracted from the data. Statistical analysis was performed using the unpaired t-test between two groups. $P < 0.05$ was considered significant. (**a:** 24h $p = 0.005$; 48 h $p < 0.001$; 72h $p < 0.001$; **b:** 24h $p = 0.001$; 48h $p = 0.0026$; 72h $p = 0.0014$ compared to the neg. control).

Further experiments were carried out in order to unfold the nature of XYLT1 induction by TGF-β1 stimulation. In initial test stimulations, no difference could be detected between one-time stimulation with 10 ng/ml TGF-β1 and two-time stimulation with 5 ng/ml TGF-β1 (data not shown).

To evaluate how long XYLT1 expression remains increased after removal of TGF-β1 from the growth medium, TGF-β/SMAD reporter K4IM cells were treated with or without TGF-β1 for 48 hours, before the supernatant was substituted by a TGF-β1 free medium. The XYLT1 expression relative to S18 was analyzed 24, 48 and 72 hours after medium exchange.

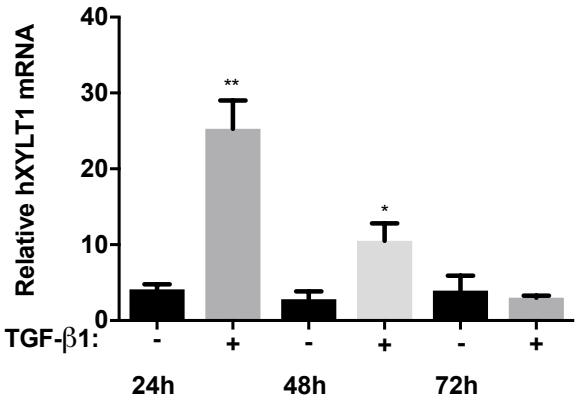

Figure 15: XYLT1 mRNA 24h, 48h and 72h after removal of TGF-β1

XYLT1 expression is still considerably elevated, 24h after removal of TGF-β1 from the growth medium. Gradual decline of XYLT1 expression after 24h: Expression is still significantly elevated compared to the control 48 h after removal, and no longer elevated 72 h after removal. K4IM cells with integrated TGF-β/SMAD reporter were grown to confluence in DMEM, without addition of FCS and penicillin/streptomycin. After one-time stimulation of the cells with, or without, 10 ng/ml TGF-β1 and incubation for 48h, the growth medium was exchanged. The cells were lysed 24h, 48h or 72h after removal of TGF-β1. RNA isolation, reverse transcription and relative quantification by qPCR was performed. Data represent steady state levels of hXYLT1-mRNA normalized to S18 RNA. 12-well plates with 60 000 cells per well and three wells per treatment group were used. Statistical analysis was performed using the unpaired t-test between two groups. $P < 0.05$ was considered significant (24h $p = 0.0052$; 48h $p = 0.0373$; 72h $p = 0.6811$ compared to the neg. control).

XYLT1 expression was elevated as compared to the control values at 24 and 48 hours after removal of TGF-β1, gradually decreasing with time and reaching normal expression levels similar to the unstimulated control 72 hours after removal of TGF-β1 (figure 15).

These results support the general hypothesis that XYLT1 induction can be actively regulated by TGF-β1, which, considering the arguments outlined in 1., strengthens the theory that there may exist an active regulation of water-free sodium storage in connective tissues.

3.3 Stimulation experiments with sodium chloride

The overall objective for the following series of experiments was to determine whether a hyperosmolar environment could be a direct trigger for increased sodium storage via induction of XYLT1 expression in fibroblast cells. Such findings could suggest that non-osmotic sodium storage could result as a direct buffer mechanism for regulating excessive extracellular sodium concentrations. To test this theory, K4IM cells with integrated NFAT5 reporter were used as detailed earlier, providing an internal control of successful NFAT5 pathway activation. The reporter cells

were treated with or without sodium chloride for 48 hours, before levels of XYLT1 mRNA were analyzed by qPCR. Stimulation with TGF-β1 was used as a positive control for induction of XYLT1 expression. Stimulation with combined sodium chloride and TGF-β1 was also performed, with the aim to uncover potential additive effects. Additionally, TGF-β3 was included in these experiments to asses if other TGF-β isoforms might have an effect on XYLT1 expression, similar to that seen with TGF-β1.

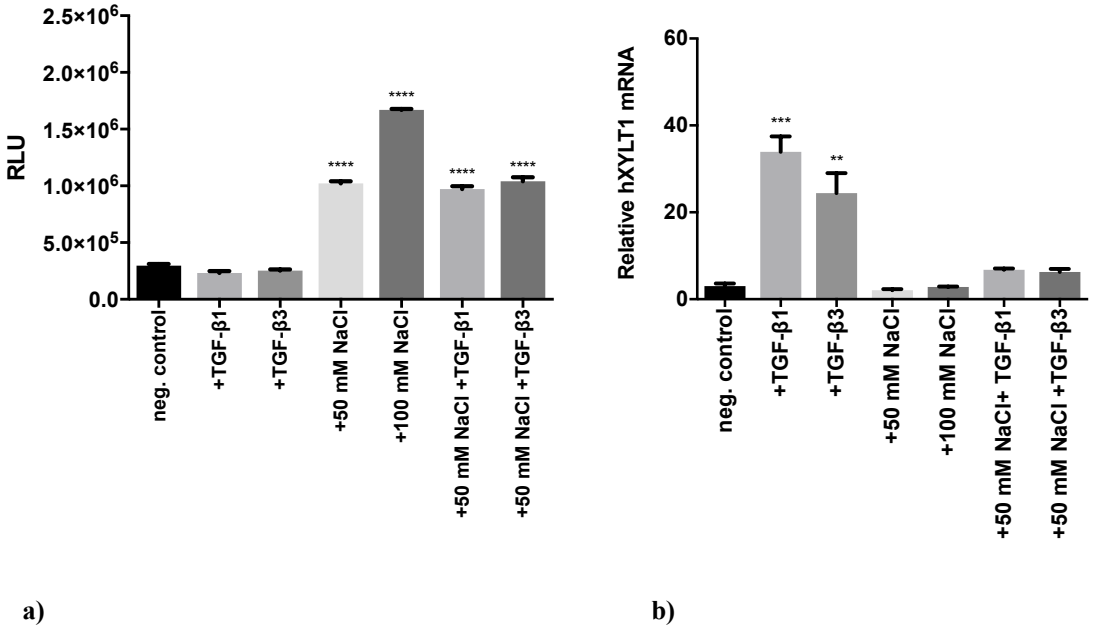

a) **b)**

Figure 16: Treatment of NFAT5 reporter K4IM cells with sodium chloride, TGFβ-1 and TGFβ-3

a) Treatment with hyperosmolar sodium chloride solutions alone, and in combination with TGFβ-1, and TGFβ-3, activated the NFAT5 reporter construct. Treatment with TGFβ-1 or TGFβ-3 alone did not lead to reporter construct activation b) XYLT1 expression was induced both by TGFβ-1 and TGFβ-3, whereas no induction by hyperosmotic stress was found. In fact, addition of sodium chloride to the treatment with TGFβ-1 and TGFβ-3 lowered their effect on XYLT1 expression. K4IM cells with integrated NFAT5 reporter were grown to confluence in DMEM, without addition of FCS and penicillin/streptomycin. Next, the cells were treated one time with 10 ng/ml TGF-β1, 10 ng/ml TGF-β3, 50 mM NaCl, 100 mM NaCl and then incubated for 24h, 48h or 72h. Reporter activity was assessed by measuring luciferase activity in the supernatant. Data are represented as relative light units (RLU). After lysis of the cells, RNA isolation, reverse transcription and relative quantification by qPCR was performed. Data represent steady state levels of hXYLT1-mRNA normalized to S18 RNA. 12-well plates with 60 000 cells per well, with three wells per treatment group were used. As a control, unstimulated K4IM cells without integrated reporter were incubated under same conditions and subtracted from the data. Molar concentrations of NaCl described here were added to the standard NaCl concentration in the growth medium. Statistical analysis was performed using the unpaired t-test between two groups. P <0.05 was considered significant (**a**: p <0,0001 compared to the neg. control; **b**: TGF-β1 p=0.001; TGF-β3 p= 0.0099 compared to the neg. control).

Successful NFAT5 pathway stimulation by sodium chloride treatment was demonstrated by the enhanced reporter activity (figure 16a). Nevertheless, hyperosmotic stress did not have a discernible effect on XYLT1 expression, contesting our hypothesis regarding this question. TGF-β3 was further shown to have an equally strong induction of XYLT1 expression as was found with TGF-β1. Interestingly, the addition of sodium chloride to both TGF-β1 and TGF-β3 led to a decrease in steady state expression of XYLT1 mRNA (figure 16b). These findings contradict the theory that hyperosmolar environment functions as a direct trigger for increase of sodium storage, raising the question if there are more complex mechanisms regulating induction of XYLT1 expression, and sodium storage during hyperosmotic stress.

With that background, the potential effects of sodium chloride treatment on TGF-β expression was then studied, under the hypothesis that TGF-β induction in response to osmotic stress may function as a link between a hyperosmolar environment and increased XYLT1 activity.

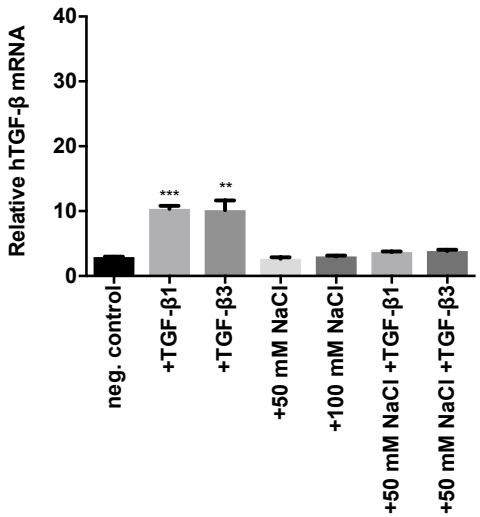

Figure 17: TGF-β mRNA after treatment with sodium chloride, TGFβ-1 and TGFβ-3

TGF-β mRNA expression in NFAT5 reporter K4IM cells could not be induced by hyperosmotic stress. Data represent steady state levels of TGF-β-mRNA normalized to S18 RNA. qPCR was performed on the samples generated in the stimulation experiment described in the figure 16, refer to there for detailed information. Statistical analysis was performed using the unpaired t-test between two groups. P <0.05 was considered significant (TGF-β1 p=0.0001; TGF-β3 p= 0.0082 compared to the neg. control).

The results showed no differences in TGF-β expression, with or without hyperosmotic stress, while, as expected, induction of TGF-β expression by TGFβ-1 or TGFβ-3 stimulation was found (figure 17). This data suggests, that TGF-β alone is not the link between hyperosmotic stress and regulation of sodium storage. We therefore concluded that more complex mechanisms than previously postulated such as the presence of endocrine regulators may be necessary for induction of XYLT1 expression by fibroblast cells.

3.4 Stimulation experiments with endocrine regulators involved in sodium and phosphate homeostasis

Since we were not able to induce XYLT1 expression by osmotic stress in the *in vitro* experiments described above, endocrine regulators involved in sodium and phosphate homeostasis were chosen for a series of stimulation experiments, in the search for other stimuli than TGF-β, capable of inducing XYLT1 expression.

3.4.1 Treatment with AVP

As a first candidate, arginine vasopressin (AVP) was tested. As it is known to be a key mediator in maintaining plasma osmolality, we hypothesized, that it may play a role in internal sodium balance, regulating the exchange between sodium linked to body water and sodium bound to proteoglycans via XYLT1. Based on an earlier study, examining the treatment of isolated rat cardiac fibroblasts with AVP, (Yang, Zhao, Zheng, & Li, 2003), potential concentrations of AVP were established for our *in vitro* stimulation experiment. To test our theory, K4IM cells with integrated TGF-β/SMAD reporter were treated with AVP for 48 hours before levels of XYLT1 mRNA were analyzed by qPCR. Treatment with TGF-β1, with and without addition of AVP, was included in the experiment, allowing for discovery of potential additive effects.

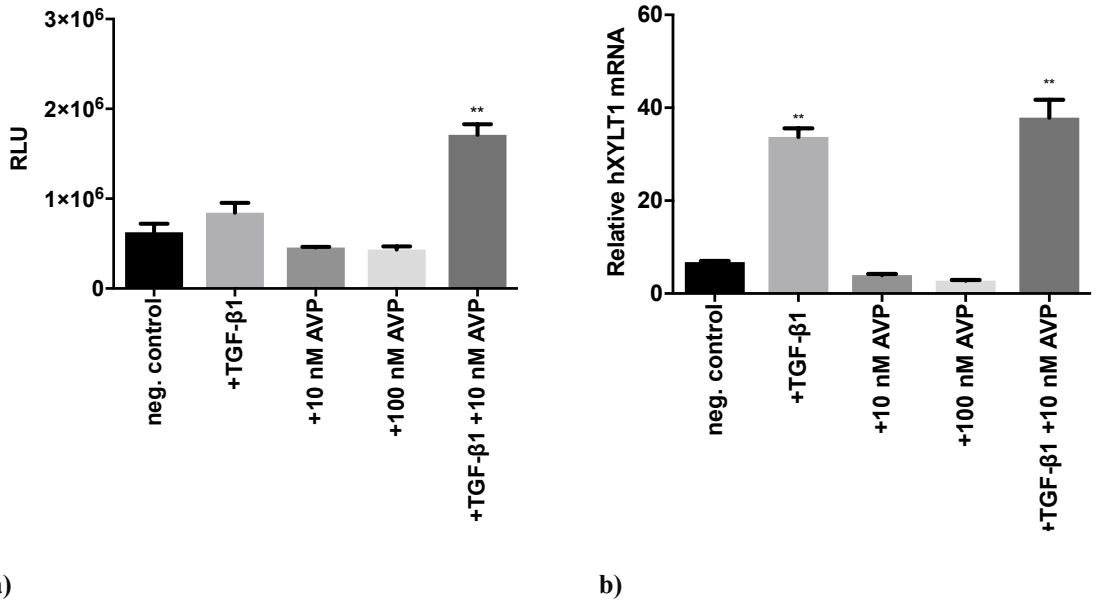

a) **b)**

Figure 18: Treatment of TGF-β/SMAD reporter K4IM cells with AVP and TGFβ-1

a) Sole treatment with arginine vasopressin (AVP) did not increase activation of the TGF-β/SMAD reporter construct, while synergistic effects of combined treatment with AVP and TGF-β1 were found. b) XYLT1 expression was neither induced by AVP in sole treatment, nor through synergistic effects with TGF-β1. TGF-β1 was used as positive control. Cells were stimulated with either 10 ng/ml TGF-β1, 10 nM AVP, 100 nM AVP or 10 ng/ml TGF-β1+10 nM AVP. After 48 h incubation, reporter activity was assessed by measuring luciferase activity in the supernatant. Data are represented as relative light units (RLU). After lysis of the cells, RNA isolation, reverse transcription and relative quantification by qPCR was performed. Data represent steady state levels of hXYLT1-mRNA normalized to S18 RNA. 12-well plates with 60 000 cells per well, with three wells per treatment group were used. As a control, unstimulated not transfected K4IM cells were incubated under same conditions and subtracted from the data. Statistical analysis was performed using the unpaired t-test between two groups. $P < 0.05$ was considered significant (**a**: TGF-β1+AVP p=0.0075; **b**: TGF-β1 p= 0.0014; TGF-β1+AVP p= 0.0082 compared to the neg. control).

Once again, TGF-β1 was shown to strongly induce XYLT1 expression. However, no effect of AVP treatment on the expression of XYLT1 could be identified in this model (figure 18b). One interpretation of these results is that AVP either has no role in regulation of XYLT1 expression, or that dermal fibroblasts are not the optimal choice of cell type for studying AVP stimulation, and that other cells known to be more responsive to AVP, e.g. vascular smooth muscle cells, would be a more suitable choice to investigate this matter.

Although it is without relevance for the theory that AVP is actively regulating sodium storage via XYLT1, it is noteworthy that combined treatment with AVP and TGF-β1 led to significantly

stronger activation of the TGF-β/SMAD reporter construct than sole treatment with TGF-β1, suggesting additive effects, while AVP alone could not increase activation of the TGF-β/SMAD reporter construct (figure 18a).

3.4.2 Treatment with ET-1 and FGF23

As a further expansion of our search for potential regulators of XYLT1 expression, a second stimulation experiment was carried out, in which the effects of fibroblast growth factor 23 (FGF23) and Endothelin 1 (ET-1) on XYLT1 expression were studied.

FGF23 acts as an important mediator in phosphate homeostasis and is known to be dramatically elevated in chronic kidney disease (Olauson & Larsson, 2013). We hypothesized that it might work as a link between decreased renal function, altered renal phosphate handling and exchange of sodium storage.

ET-1 on the other hand, is shown to be involved in the response to high salt intake, and to facilitate movement of Na^+ through skin interstitium (Speed et al., 2015). Thus it is possible that ET-1 could directly influence the regulation of sodium storage in arteries and skin. In earlier studies, ET-1 was shown to bind to dermal fibroblasts through specific high affinity surface receptors (Falanga, Katz, Kirsner, & Alvarez, 1992), and therefore seemed well suitable for our *in vitro* model.

In the following experiment, K4IM reporter cells with integrated TGF-β/SMAD reporter were treated with FGF23 and ET-1, respectively, for 48 hours. Then, levels of XYLT1 mRNA were analyzed by qPCR. Sole treatment with TGF-β1 and TGF-β3, and treatment with TGF-β1 in combination with FGF23 and ET-1, respectively, was included in the experiment as a positive control for induction of XYLT1 expression and allowing for the study of potential synergistic effects. As in previous experiments, the TGF-β/SMAD pathway could be monitored by the reporter construct.

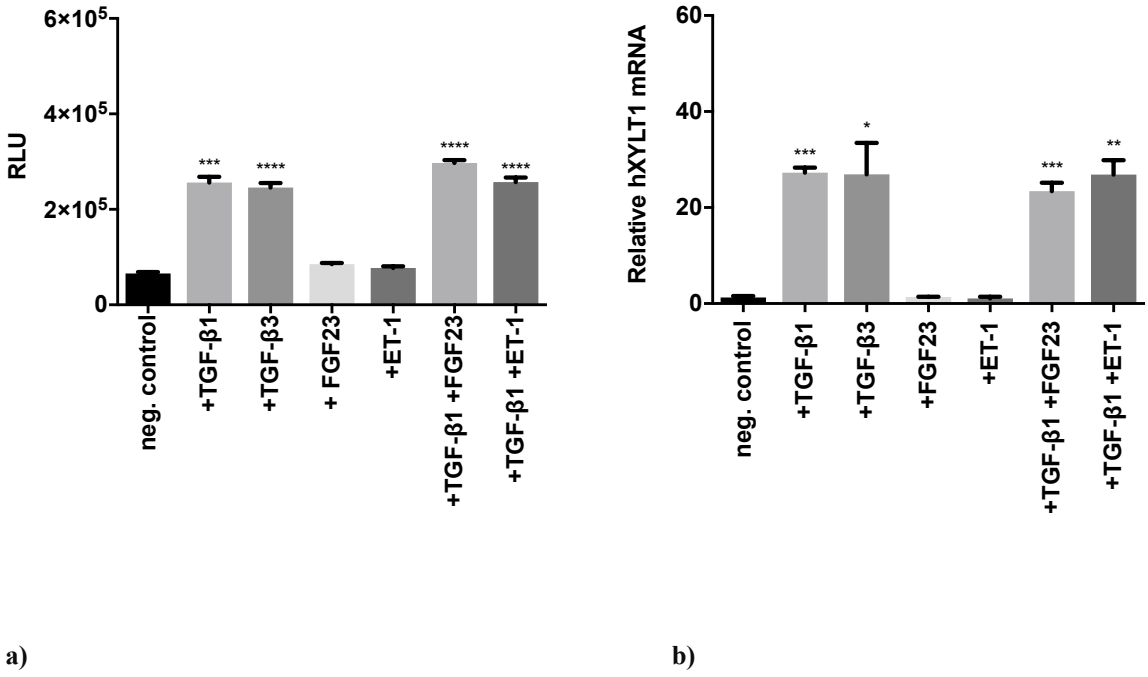

a) **b)**

Figure 19: Treatment of TGF-β/SMAD reporter K4IM cells with ET-1, FGF23, TGFβ-1 and TGFβ-3

a) Sole treatment with ET-1 and FGF23, respectively, did not increase activation of the TGF-β/SMAD reporter construct, and no synergistic effects on the pathway were found by combined treatment with TGF-β1. b) XYLT1 expression could not be induced by sole treatment with ET-1 or FGF23, and no synergistic effects in combination with TGF-β1 on XYLT1 expression were found. TGF-β1 and TGF-β3 functioned as positive control. K4IM cells with integrated TGFβ/SMAD reporter were grown to confluence in DMEM, without addition of FCS and penicillin/streptomycin. Next, the cells were stimulated one time with either 10 ng/ml TGF-β1, 10 ng/ml TGF-β3, 1 µg/ml FGF23 or 100 mM ET-1 and incubated for 48h. Then, reporter activity was assessed by measuring luciferase activity in the supernatant. Data are represented as relative light units (RLU). After lysis of the cells, RNA isolation, reverse transcription and relative quantification by qPCR was performed. Data represent steady state levels of hXYLT1-mRNA normalized to S18 RNA. 12-well plates with 60 000 cells per well, with three wells per treatment group were used. As a control, unstimulated not transfected K4IM cells were incubated under same conditions and subtracted from the data. Statistical analysis was performed using the unpaired t-test between two groups. P <0,05 was considered significant (**a**: p<0.0001 compared to the neg. control, **b**: TGF-β1 p< 0.0001; TGF-β3 p= 0.0136; TGF-β1+FGF23 p= 0.0002; TGF-β1+ET-1 p= 0.0010 compared to the neg. control).

No differences to the control in XYLT1 mRNA could be detected after ET-1 and FGF23 treatment, respectively, while the positive control with TGF-β1 and TGF-β3 showed increased activation of the TGF-β/SMAD pathway and induction of XYLT1 expression. No additive effect of combined treatment nor significant activation of the TGF-β/SMAD pathway by ET-1 or FGF23

was seen (figure 19b). Since the stimulation with ET-1 and FGF23 did not lead to increased XYLT1 activity, their role in regulation of sodium storage remains for the most part unknown.

3.5 CHSY1 and CHPF2, enzymes involved in GAG biosynthesis

While most of the external stimuli tested in our experiments were unable to induce XYLT1 expression, it was shown repetitively, that TGF-β1 strongly induces XYLT1 expression. In order to study if other genes involved in GAG synthesis could be induced by TGF-β1 stimulation, two genes engaged in chondroitin polymerization, CHSY1 and CHPF, were tested, as they play an important role in biosynthesis of chondroitin sulfate. CHSY1 is a gene encoding for chondroitin sulfate synthase 1, a member of the chondroitin N-acetylgalactosaminyltransferase family, and was in an earlier study shown to be induced by TGF-β1 in nucleus pulposus cells in rats (Hu et al., 2015). Chondroitin polymerizing factor (CHPF), also known as CSS2 or CHSY2, encodes for chondroitin sulfate synthase 2 (Yada et al., 2003).

CHSY1 and CHPF gene expression was analyzed by qPCR in the samples generated in the TGF-β1 stimulation experiment (refer to 3.2.).

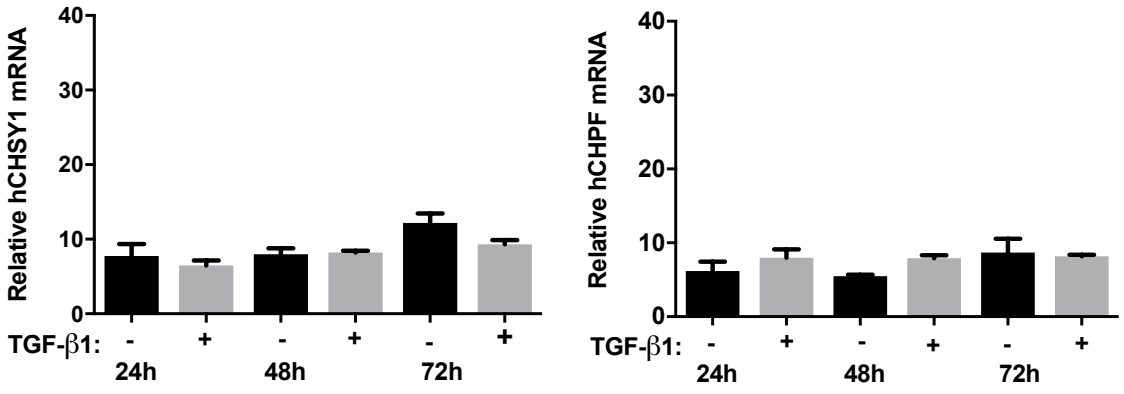

Figure 20: CHSY1 and CHPF mRNA after treatment with TGF-β1

Treatment with TGF-β1 did no show induction of CHSY1 (a) or CHPF (b) expression in K4IM TGF-β/SMAD reporter cells after 24h, 48h and 72h incubation. Data represent steady state levels of hCHSY1-mRNA and hCHPF-mRNA normalized to S18 RNA. qPCR was performed on the samples generated in the stimulation experiment described in 3.2. Please refer to figure 14 for detailed information.

While mRNA levels were established for both enzymes, no differences in expression of CHSY1 and CHPF could be detected by treatment with TGF-β1 (figure 20), suggesting that GAG expression induced by TGF-β1 is largely dependent on the activation of the key enzyme XYLT1 and that this first enzyme in the pathway of GAG biosynthesis represents a potential key regulator for sodium storage.

4 Discussion

4.1 Overview of this work

High correlation between tissue sodium concentrations, glycosaminoglycan content and the expression of XYLT1, the enzyme initiating glycosaminoglycan synthesis, was described in a recent study. The goal of the present study was to identify potential stimuli that modulate XYLT1 expression in fibroblast cells to better characterize XYLT1 biology in connective tissues- a putative source for sodium storage.

As a first step, we established systems to monitor pathway activation status in human fibroblasts, functioning as internal controls of activation of the TGF-β and hyperosmotic stress signaling pathways. These tools could also serve as internal controls for future stimulation experiments, and could be helpful for studying alterations in homeostatic pathways.

In the next step, the reporter-engineered cells were used in a series of stimulation experiments, where the reporter construct served as an internal control for successful pathway stimulation. XYLT1 mRNA expression was quantified by real-time PCR.

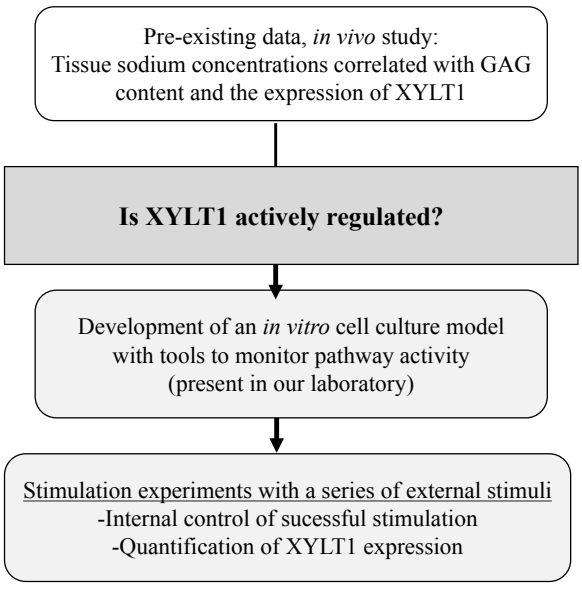

Figure 21: Experimental outline

We observed induction of XYLT1 mRNA expression in fibroblast cells by treatment with TGF-β1 and TGF-β3. Media with hypertonic sodium, elevated Vasopressin, Endothelin-1 and FGF23 concentrations, respectively, did not have significant effect on XYLT1 expression. Our data support the hypothesis that XYLT1 is actively regulated by TGF-β in fibroblasts, which strengthens the theory that there is active regulation of water-free sodium storage. Because upregulated TGF-β1 in kidney disease is shown to contribute to progression of renal fibrosis, it may represent the link between renal disease, elevated GAG synthesis and Na^+ excess in tissue as a consequence thereof.

4.2 Relevance of water-free sodium storage

Osmotically inactive sodium storage pools exist without doubt (Titze, 2014), and incorporation of sodium into glycosaminoglycans has been proposed (Mobasheri, 1998). However, the biological processes of these pools and their relevance for disease remain unclear.

4.2.1 Exchangeability of sodium pools

Regarding the potential biology underlying these processes, it is of central importance to determine whether the size of the sodium storage pools is constant, or can change under varying conditions. There is evidence that the sodium pools are exchangeable, as changes in tissue Na^+ content could be demonstrated under varying study conditions. For example, a mobilization of sodium storage is seen during starvation (Garnett, Ford, Golding, Mardell, & Whyman, 1968), and tissue Na^+ content has been shown to decrease in hypertensive patients with primary hyperaldosteronism after operative or spironolactone treatment (C. Kopp et al., 2012).

4.2.2 The potential biology behind this process

Assuming an exchangeability of sodium storage, a natural question to ask, is what conditions lead to shifts in the amount of non-osmotically bound sodium. Schafflhuber et al. (2007) proposed that Na^+ tissue content varies as a response to states of sodium retention or loss and suggested that sodium storage pools play a role in the regulation of plasma volume and blood pressure. With this in mind, it is possible that sodium storage may function as a buffer to help compensate for an imbalance between sodium in- and output. A different perspective on the potential mechanisms driving sodium storage was postulated by Wiig et al. (2013), suggesting that an increase in Na^+ tissue content is linked to the activation of the immune system, and ultimately leads to increased sodium clearance through the skin.

4.2.3 Physiological phenomenon or related to disease?

Whether sodium storage is a physiological response or related to disease is a controversial topic. On the one hand, Fischereder et al. (2017) and Dahlmann et al. (2015) have suggested that it may respresent an individual physiological response, rather then a component or process associated with progressive kidney disease. In their studies, no difference in tissue sodium content was found between dialysis patients and healthy controls. Instead, a high interindividual variation and age dependency of tissue Na^+ content that correlated with increasing age was observed.

By contrast, Schneider et al. (2017) have suggested that Na^+ excess may contribute to cardiovascular morbidity in CKD, as a correlation of skin sodium concentrations with left ventricular mass in patients with chronic kidney disease was found. Supporting this, osmotically inactive Na^+ storage was suggested to contribute to the development of salt sensitive hypertension (Titze, Krause, et al., 2002).

We speculate that the pathophysiology behind these observations, could in part be explained by the following: the GAG content in arteries was shown to correlate with tissue Na^+ content in arteries (Fischereder et al., 2017). The accumulation of proteoglycans in the vascular wall correlates with hypertension, and glycosaminoglycan overproduction has been shown to be associated with increased aortic calcification (Purnomo et al., 2013). It could then be suggested that Na^+ excess may represent a trigger for vascular stiffening and hypertension, and microvascular disease as a consequence. An additional question in this regard is whether sodium incorporation into GAGs could change the mechanical properties of GAGs, reinforcing the stiffening of arterial walls.

To gain insight into this topic, it would be of interest to extend the study of Schneider et al. (2017) by investigating correlation of left ventricular mass not only with Na^+ content in the skin, but also with tissue Na^+ content in arteries.

An alternate interpretation of the observations described by Schneider et al. (2017) and Titze, Krause, et al. (2002) is that they may be describing essentially a saturated physiological Na^+ buffer linked to an active regulation of sodium storage a process seen after compensating for high serum sodium concentrations through storing sodium over time, as a means of preventing hypertension.

4.2.4 Intervening sodium storage - a way to prevent disease in the future?

Whether sodium storage is a physiological phenomenon or a part of disease, it may represent a way of preventing disease; Either through supporting a normal physiological process, or through inhibiting a pathophysiological process. Therefore, the study of the regulatory mechanisms of sodium storage via the regulation of a gene like XYLT1, which encodes for the first enzyme in

the committed biosynthesis of GAGs, could provide information and potentially targets for clinical intervention, e.g. to reduce Na^+ tissue content in patients with cardiovascular disease or renal disease, if Na^+ excess is a factor for progression of the disease.

4.3 TGF-β - possible link between renal disease and increased sodium storage?

The role of canonical TGF-β signaling pathways in the regulation of non-osmotic sodium storage is not well understood. In our *in vitro* study detailed here, XYLT1 mRNA expression was shown to be strongly inducible by TGF-β1 and TGF-β3. This observation supports previous studies, where TGF-β was shown to modulate XYLT1 expression *in vitro* (Fischereder et al., 2017), (Faust et al., 2013). While Faust et al. (2013) interpreted this observation in context of the pathology of skin fibrosis and fibrotic remodeling, we propose that regulation of sodium storage by TGF-β1 via XYLT1 may also be directly linked to increased tissue Na^+ content (Fischereder et al., 2017).

TGF-β1 is associated with kidney disease and shown to contribute to the progression of renal fibrosis (Meng, Nikolic-Paterson, & Lan, 2016). It may also provide a link between renal disease, elevated GAG synthesis and Na^+ storage in tissues. We propose that TGF-β signaling may be working in a paracrine manner in this context, e.g. through release from endothelial cells, rather than through a systemic elevation of TGF-β levels.

4.4 Another look at XYLT1

4.4.1 XYLT1 – a key enzyme regulating sodium storage

Study of the regulation of XYLT1 regulation was the main subject of this thesis. This enzyme encodes for a protein that appears to represent the rate-limiting step in the biosynthesis of GAGs. These structures have been suggested to provide a structure for non-osmotic sodium storage in tissues. Elevated GAG synthesis increases a negative charge density in tissues, which could lead to increased Na^+ incorporation (Titze et al., 2004).

In addition to XYLT1, we also studied the expression of other enzymes involved in GAG synthesis. Unlike a previous study, where a positive correlation between skin Na^+ content, CHSY1 expression and proteoglycan content was observed (Titze et al., 2004), we were not able to show modulation of CHSY1 or CHPF expression *in vivo* or *in vitro*. XYLT1 expression, however, was shown to be strongly inducible. Our findings support the results described by Fischereder et al. (2017) which showed altered expression of XYLT1 which positively correlated with tissue Na^+ content *in vivo*, that included the parallel evaluation of a series of genes involved in GAG synthesis, including CHSY1 and CHPF.

We therefore assume that XYLT1, known to be the rate-limiting enzyme in GAG synthesis, represents the key enzyme regulating potential sodium storage in tissues. We were able to induce XYLT1 expression in fibroblast cells by stimulation with TGF-β, suggesting that there is an active biological regulation of XYLT1 expression.

4.4.2 Consequences of XYLT1 expression

If we now assume the general importance of of XYLT1 expression in the regulation of sodium storage, one could question whether tissue sodium storage pools may change directly in response to XYLT1 expression, e.g. as seen in hereditary diseases with mutations of XYLT1, causing loss of function, or polymorphisms causing increased XYLT1 expression.

A hereditary disease, known to be caused by complete loss of function of XYLT1, is called desbuquois dysplasia type 2. It is a rare type of osteochondrodysplasia, which causes significant reduction of cellular proteoglycan content in skin fibroblasts (Bui et al., 2014). One might assume then that patients with this disease may also show a decreased tissue Na^+ content. However, no such study has been conducted to date. In order to further investigate consequences of hypoexpression of XYLT1, a XYLT1 knock-down construct was designed in our laboratory and transfected into the K4IM cells. Due to technical problems, we were not able to demonstrate functionality of the knock-down system, but with an improved construct, it could be an interesting approach in the future.

Increased XYLT expression due to polymorphisms, was identified in the heritable connective tissue disorder called pseudoxanthoma elasticum (Schon et al., 2006). The consequences of this condition in terms of sodium storage is also not reported, but in one study, no association with essential hypertension was found (Ponighaus et al., 2009).

4.5 Reporter plasmids as internal control of successful stimulation

Unfortunately, in many studies, negative results which are centrally important are also difficult to report, as it is hard to define whether it is a true negative result or a consequence of dysfunctional methods. Therefore, to avoid this problem, one of our goals was to establish a system of internal control for the treatment in dermal fibroblasts. Using reporter plasmids, we not only developed safe and well-functioning constructs to control successful stimulation, but we were also able to study possible increased activation of relevant regulatory pathways. Additional to the study of XYLT1 mRNA expression, our constructs allowed us to monitor signaling pathways, potentially relevant in the regulation of sodium storage, namely the TGF-β/SMAD pathway and the pathway for osmotic-stress response (NFAT5). The following techniques contribute to the generation of the constructs (Jackel et al., 2016):

1) The AMAXA Nucleofection was used to transfect our experimental dermal fibroblasts with the various plasmids. The system was optimized for small volumes and the specific protocol applied for the desired cell line allowed for high efficiency and good cell viability. This was very important when using the K4IM cells, as they are difficult to transfect and proliferate slowly.
2) The Sleeping Beauty transposon technology (Mates et al., 2009) allowed for stable and efficient transfections by near-random integration in the host DNA.
3) With the use of a secreted reporter protein (Gaussia luciferase), as the read-out (Tannous, Kim, Fernandez, Weissleder, & Breakefield, 2005) we were able to measure pathway activity without cell lysis before proceeding to RT-PCR. Before measurement, cell density was controlled by microscopy, as the results are not standardized to cell number.

As expected, control activation of the TGF-β/SMAD reporter by TGF-β, and of the NFAT5 reporter by hypertonic sodium during XYLT1 induction was demonstrated (see 3.2. and 3.3.), whereas no effects of most of the other stimuli were found. Interestingly, addition of AVP with TGF-β1 led to stronger activation of the pathway than did sole treatment with TGF-β1 (see 3.4.1). A link between AVP and TGF-β has been previously described in the literature: AVP was shown to induce TGF-β secretion by proliferating mesangial cells, possibly contributing to glomerulosclerosis in renal disease (Tahara, Tsukada, Tomura, Yatsu, & Shibasaki, 2008). However, the additive effects of AVP and TGF-β1 on the TGF-β/SMAD signaling pathway are not yet understood and a subject of further investigations.

Another finding that cannot be explained by our current knowledge on the topic, is that, addition of sodium chloride with TGF-β treatment lowered the effect on XYLT1 expression. Although XYLT1 expression was not inducible by treatment with hypertonic sodium, the NFAT5 reporter showed activation of the pathway, indicating successful stimulation.

The excellent functionality of our reporter engineered K4IM cells allowed them to be useful tools for future stimulation experiments and pathway studies.

4.6 Limitations of our *in vitro* model

The *in vitro* cell culture study applied here allowed for detailed and controlled analysis of the fibroblast response to various stimuli. Importantly, the results from *in vitro* experiments are not always transferable to complex organisms.

Using this system we sought to identify stimuli that modulate steady state XYLT1 mRNA expression. No effect of treatment with hypertonic sodium, AVP, FGF23 and ET-1 on XYLT1 expression was found, suggesting that they do not actively regulate GAG expression in fibroblasts.

It is possible, that effects are difficult to see in a direct *in vitro* setting, as these processes could work in other cell settings or through complex interactions between several cell types and local mediators *in vivo.* In this regard, it is interesting that XYLT1 expression correlated with calculated osmolality *in vivo* in skin, muscle and arteries (Fischereder et al., 2017). The regulators tested in our study were not directly measured in the previous *in vivo* study.

Sodium storage is suggested to take place in different tissues such as skin, muscle and arteries, and models with other cell types present in these tissues would be useful to study the regulation of sodium storage. For example, co-culture experiments with our reporter engineered fibroblasts and endothelial cells could be an interesting system to re-evaluate the potential effects of these agents.

4.7 Outlook: Quantification of sodium concentrations and GAG content *in vitro*

To further strengthen our theory, the next intuitive step is to investigate the potential correlation between XYLT1 expression, sodium concentration and GAG content *in vitro.*

Relevant question in this topic include:

1) Quantification of sodium concentrations *in vitro*: For example experiments using radioactive sodium to measure changes in sodium content *in vitro* (in cooperation with the institute of Pharmaceutical Radiochemistry, Technische Universität München).
2) Quantification of GAG content *in vitro*: Either by using a suitable glycosaminoglycan antibody (FACS) or by developing an appropriate staining method.
3) Establishment of a functioning XYLT1 knock-down construct to investigate consequences of reduced XYLT1 expression on sodium concentrations.
4) Expansion of the *in vitro* experiments with a broader range of cell types, by using e.g. endothelial cells.
5) Study of the effect of the endocrine regulators AVP, FGF23 and ET-1 on XYLT1 expression *in vivo* e.g. in human studies or animal studies.

5 References

Aramburu, J., Drews-Elger, K., Estrada-Gelonch, A., Minguillon, J., Morancho, B., Santiago, V., & Lopez-Rodriguez, C. (2006). Regulation of the hypertonic stress response and other cellular functions by the Rel-like transcription factor NFAT5. *Biochem Pharmacol, 72*(11), 1597-1604. doi:10.1016/j.bcp.2006.07.002

Barberis, C., Mouillac, B., & Durroux, T. (1998). Structural bases of vasopressin/oxytocin receptor function. *J Endocrinol, 156*(2), 223-229.

Brunner, A., Kolarich, D., Voglmeir, J., Paschinger, K., & Wilson, I. B. (2006). Comparative characterisation of recombinant invertebrate and vertebrate peptide O-Xylosyltransferases. *Glycoconj J, 23*(7-8), 543-554. doi:10.1007/s10719-006-7633-z

Bui, C., Huber, C., Tuysuz, B., Alanay, Y., Bole-Feysot, C., Leroy, J. G., . . . Cormier-Daire, V. (2014). XYLT1 Mutations in Desbuquois Dysplasia Type 2. *American Journal of Human Genetics, 94*(3), 405-414. doi:10.1016/j.ajhg.2014.01.020

Chen, S., Iglesias-de la Cruz, M. C., Jim, B., Hong, S. W., Isono, M., & Ziyadeh, F. N. (2003). Reversibility of established diabetic glomerulopathy by anti-TGF-beta antibodies in db/db mice. *Biochem Biophys Res Commun, 300*(1), 16-22.

Christoph, K., Beck, F. X., & Neuhofer, W. (2007). Osmoadaptation of Mammalian cells - an orchestrated network of protective genes. *Curr Genomics, 8*(4), 209-218.

Cuellar, K., Chuong, H., Hubbell, S. M., & Hinsdale, M. E. (2007). Biosynthesis of chondroitin and heparan sulfate in chinese hamster ovary cells depends on xylosyltransferase II. *J Biol Chem, 282*(8), 5195-5200. doi:10.1074/jbc.M611048200

Dahlmann, A., Dorfelt, K., Eicher, F., Linz, P., Kopp, C., Mossinger, I., . . . Titze, J. M. (2015). Magnetic resonance-determined sodium removal from tissue stores in hemodialysis patients. *Kidney Int, 87*(2), 434-441. doi:10.1038/ki.2014.269

Derynck, R., & Zhang, Y. E. (2003). Smad-dependent and Smad-independent pathways in TGF-beta family signalling. *Nature, 425*(6958), 577-584. doi:10.1038/nature02006

Falanga, V., Katz, M. H., Kirsner, R., & Alvarez, A. F. (1992). The effects of endothelin-1 on human dermal fibroblast growth and synthetic activity. *J Surg Res, 53*(5), 515-519.

Farber, S. J. (1960). Mucopolysaccharides and sodium metabolism. *Circulation, 21*, 941-947.

Faust, I., Roch, C., Kuhn, J., Prante, C., Knabbe, C., & Hendig, D. (2013). Human xylosyltransferase-I - a new marker for myofibroblast differentiation in skin fibrosis. *Biochem Biophys Res Commun, 436*(3), 449-454. doi:10.1016/j.bbrc.2013.05.125

Finnson, K. W., McLean, S., Di Guglielmo, G. M., & Philip, A. (2013). Dynamics of Transforming Growth Factor Beta Signaling in Wound Healing and Scarring. *Adv Wound Care (New Rochelle), 2*(5), 195-214. doi:10.1089/wound.2013.0429

Fischereder, M., Michalke, B., Schmockel, E., Habicht, A., Kunisch, R., Pavelic, I., . . . Stangl, M. (2017). Sodium storage in human tissues is mediated by glycosaminoglycan expression. *Am J Physiol Renal Physiol, 313*(2), F319-F325. doi:10.1152/ajprenal.00703.2016

Fukagawa, M., Nii-Kono, T., & Kazama, J. J. (2005). Role of fibroblast growth factor 23 in health and in chronic kidney disease. *Curr Opin Nephrol Hypertens, 14*(4), 325-329.

Garnett, E. S., Ford, J., Golding, P. L., Mardell, R. J., & Whyman, A. E. (1968). The mobilizaton of osmotically inactive sodium during total starvation in man. *Clin Sci, 35*(1), 93-103.

Grabner, A., Amaral, A. P., Schramm, K., Singh, S., Sloan, A., Yanucil, C., . . . Faul, C. (2015). Activation of Cardiac Fibroblast Growth Factor Receptor 4 Causes Left Ventricular Hypertrophy. *Cell Metab, 22*(6), 1020-1032. doi:10.1016/j.cmet.2015.09.002

Heer, M., Baisch, F., Kropp, J., Gerzer, R., & Drummer, C. (2000). High dietary sodium chloride consumption may not induce body fluid retention in humans. *Am J Physiol Renal Physiol, 278*(4), F585-595.

Hiyama, A., Gajghate, S., Sakai, D., Mochida, J., Shapiro, I. M., & Risbud, M. V. (2009). Activation of TonEBP by calcium controls {beta}1,3-glucuronosyltransferase-I expression, a key regulator of glycosaminoglycan synthesis in cells of the intervertebral disc. *J Biol Chem, 284*(15), 9824-9834. doi:10.1074/jbc.M807081200

Hu, B., Shi, C., Tian, Y., Zhang, Y., Xu, C., Chen, H., . . . Yuan, W. (2015). TGF-beta Induces Up-Regulation of Chondroitin Sulfate Synthase 1 (CHSY1) in Nucleus Pulposus Cells Through MAPK Signaling. *Cell Physiol Biochem, 37*(2), 793-804. doi:10.1159/000430396

Huang, X. R., Chung, A. C., Wang, X. J., Lai, K. N., & Lan, H. Y. (2008). Mice overexpressing latent TGF-beta1 are protected against renal fibrosis in obstructive kidney disease. *Am J Physiol Renal Physiol, 295*(1), F118-127. doi:10.1152/ajprenal.00021.2008

Ivanova, L. N., Archibasova, V. K., & Shterental, I. (1978). [Sodium-depositing function of the skin in white rats]. *Fiziol Zh SSSR Im I M Sechenova, 64*(3), 358-363.

Jackel, C., Nogueira, M. S., Ehni, N., Kraus, C., Ranke, J., Dohmann, M., . . . Nelson, P. J. (2016). A vector platform for the rapid and efficient engineering of stable complex transgenes. *Sci Rep, 6*, 34365. doi:10.1038/srep34365

Jantsch, J., Binger, K. J., Muller, D. N., & Titze, J. (2014). Macrophages in homeostatic immune function. *Front Physiol, 5*, 146. doi:10.3389/fphys.2014.00146

Kam, P. C., Williams, S., & Yoong, F. F. (2004). Vasopressin and terlipressin: pharmacology and its clinical relevance. *Anaesthesia, 59*(10), 993-1001. doi:10.1111/j.1365-2044.2004.03877.x

Khalil, N. (1999). TGF-beta: from latent to active. *Microbes Infect, 1*(15), 1255-1263.

Kiela, P. R., & Ghishan, F. K. (2009). Recent advances in the renal–skeletal–gut axis that controls phosphate homeostasis. *Lab Invest, 89*(1), 7-14. doi:10.1038/labinvest.2008.114

Kino, T., Takatori, H., Manoli, I., Wang, Y., Tiulpakov, A., Blackman, M. R., . . . Segars, J. H. (2009). Brx mediates the response of lymphocytes to osmotic stress through the activation of NFAT5. *Sci Signal, 2*(57), ra5. doi:10.1126/scisignal.2000081

Kohan, D. E., Inscho, E. W., Wesson, D., & Pollock, D. M. (2011). Physiology of endothelin and the kidney. *Compr Physiol, 1*(2), 883-919. doi:10.1002/cphy.c100039

Kopp, C., Linz, P., Wachsmuth, L., Dahlmann, A., Horbach, T., Schofl, C., . . . Titze, J. (2012). (23)Na magnetic resonance imaging of tissue sodium. *Hypertension, 59*(1), 167-172. doi:10.1161/HYPERTENSIONAHA.111.183517

Kopp, J. B., Factor, V. M., Mozes, M., Nagy, P., Sanderson, N., Bottinger, E. P., . . . Thorgeirsson, S. S. (1996). Transgenic mice with increased plasma levels of TGF-beta 1 develop progressive renal disease. *Lab Invest, 74*(6), 991-1003.

Kubiczkova, L., Sedlarikova, L., Hajek, R., & Sevcikova, S. (2012). TGF-beta - an excellent servant but a bad master. *J Transl Med, 10*, 183. doi:10.1186/1479-5876-10-183

Kuhn, J., Gotting, C., Schnolzer, M., Kempf, T., Brinkmann, T., & Kleesiek, K. (2001). First isolation of human UDP-D-xylose: proteoglycan core protein beta-D-xylosyltransferase secreted from cultured JAR choriocarcinoma cells. *J Biol Chem, 276*(7), 4940-4947. doi:10.1074/jbc.M005111200

Lindahl, U., Couchman, J., Kimata, K., & Esko, J. D. (2015). Proteoglycans and Sulfated Glycosaminoglycans. In A. Varki, R. D. Cummings, J. D. Esko, P. Stanley, G. W. Hart, M. Aebi, A. G. Darvill, T. Kinoshita, N. H. Packer, J. H. Prestegard, R. L. Schnaar, & P. H. Seeberger (Eds.), *Essentials of Glycobiology*. Cold Spring Harbor (NY): Cold Spring Harbor Laboratory Press

Loeffler, I., & Wolf, G. (2014). Transforming growth factor-beta and the progression of renal disease. *Nephrol Dial Transplant, 29 Suppl 1*, i37-i45. doi:10.1093/ndt/gft267

Massague, J. (1998). TGF-beta signal transduction. *Annu Rev Biochem, 67*, 753-791. doi:10.1146/annurev.biochem.67.1.753

Mates, L., Chuah, M. K., Belay, E., Jerchow, B., Manoj, N., Acosta-Sanchez, A., . . . Izsvak, Z. (2009). Molecular evolution of a novel hyperactive Sleeping Beauty transposase enables robust stable gene transfer in vertebrates. *Nat Genet, 41*(6), 753-761. doi:10.1038/ng.343

Meng, X. M., Nikolic-Paterson, D. J., & Lan, H. Y. (2016). TGF-beta: the master regulator of fibrosis. *Nat Rev Nephrol, 12*(6), 325-338. doi:10.1038/nrneph.2016.48

Mieda, M., Ono, D., Hasegawa, E., Okamoto, H., Honma, K., Honma, S., & Sakurai, T. (2015). Cellular clocks in AVP neurons of the SCN are critical for interneuronal coupling regulating circadian behavior rhythm. *Neuron, 85*(5), 1103-1116. doi:10.1016/j.neuron.2015.02.005

Mittl, P. R., Priestle, J. P., Cox, D. A., McMaster, G., Cerletti, N., & Grutter, M. G. (1996). The crystal structure of TGF-beta 3 and comparison to TGF-beta 2: implications for receptor binding. *Protein Sci, 5*(7), 1261-1271. doi:10.1002/pro.5560050705

Miyakawa, H., Woo, S. K., Dahl, S. C., Handler, J. S., & Kwon, H. M. (1999). Tonicity-responsive enhancer binding protein, a rel-like protein that stimulates transcription in response to hypertonicity. *Proc Natl Acad Sci U S A, 96*(5), 2538-2542.

Mobasheri, A. (1998). Correlation between [Na+], [glycosaminoglycan] and Na+/K+ pump density in the extracellular matrix of bovine articular cartilage. *Physiol Res, 47*(1), 47-52.

Muller, S., Schottler, M., Schon, S., Prante, C., Brinkmann, T., Kuhn, J., . . . Kleesiek, K. (2005). Human xylosyltransferase I: functional and biochemical characterization of cysteine residues required for enzymic activity. *Biochem J, 386*(Pt 2), 227-236. doi:10.1042/bj20041206

Neuhofer, W. (2010). Role of NFAT5 in inflammatory disorders associated with osmotic stress. *Curr Genomics, 11*(8), 584-590. doi:10.2174/138920210793360961

Olauson, H., & Larsson, T. E. (2013). FGF23 and Klotho in chronic kidney disease. *Curr Opin Nephrol Hypertens, 22*(4), 397-404. doi:10.1097/MNH.0b013e32836213ee

Pollock, D. M., & Pollock, J. S. (2001). Evidence for endothelin involvement in the response to high salt. *Am J Physiol Renal Physiol, 281*(1), F144-150.

Ponighaus, C., Speirs, H. J., Morris, B. J., Kuhn, J., Kleesiek, K., & Gotting, C. (2009). Xylosyltransferase gene variants and their role in essential hypertension. *Am J Hypertens, 22*(4), 432-436. doi:10.1038/ajh.2009.4

Prydz, K., & Dalen, K. T. (2000). Synthesis and sorting of proteoglycans. *J Cell Sci, 113 Pt 2*, 193-205.

Purnomo, E., Emoto, N., Nugrahaningsih, D. A., Nakayama, K., Yagi, K., Heiden, S., . . . Hirata, K. (2013). Glycosaminoglycan overproduction in the aorta increases aortic calcification in murine chronic kidney disease. *J Am Heart Assoc, 2*(5), e000405. doi:10.1161/jaha.113.000405

Schafflhuber, M., Volpi, N., Dahlmann, A., Hilgers, K. F., Maccari, F., Dietsch, P., . . . Titze, J. (2007). Mobilization of osmotically inactive Na+ by growth and by dietary salt restriction in rats. *Am J Physiol Renal Physiol, 292*(5), F1490-1500. doi:10.1152/ajprenal.00300.2006

Schneider, M. P., Raff, U., Kopp, C., Scheppach, J. B., Toncar, S., Wanner, C., . . . Eckardt, K. U. (2017). Skin Sodium Concentration Correlates with Left Ventricular Hypertrophy in CKD. *J Am Soc Nephrol, 28*(6), 1867-1876. doi:10.1681/asn.2016060662

Schon, S., Schulz, V., Prante, C., Hendig, D., Szliska, C., Kuhn, J., . . . Gotting, C. (2006). Polymorphisms in the xylosyltransferase genes cause higher serum XT-I activity in patients with pseudoxanthoma elasticum (PXE) and are involved in a severe disease course. *J Med Genet, 43*(9), 745-749. doi:10.1136/jmg.2006.040972

Shimada, T., Hasegawa, H., Yamazaki, Y., Muto, T., Hino, R., Takeuchi, Y., . . . Yamashita, T. (2004). FGF-23 is a potent regulator of vitamin D metabolism and phosphate homeostasis. *J Bone Miner Res, 19*(3), 429-435. doi:10.1359/jbmr.0301264

Speed, J. S., Heimlich, J. B., Hyndman, K. A., Fox, B. M., Patel, V., Yanagisawa, M., . . . Pollock, D. M. (2015). Endothelin-1 as a master regulator of whole-body Na+ homeostasis. *Faseb j, 29*(12), 4937-4944. doi:10.1096/fj.15-276584

Sterns, R. H. (2015). Disorders of plasma sodium--causes, consequences, and correction. *N Engl J Med, 372*(1), 55-65. doi:10.1056/NEJMra1404489

Stoolmiller, A. C., Horwitz, A. L., & Dorfman, A. (1972). Biosynthesis of the chondroitin sulfate proteoglycan. Purification and properties of xylosyltransferase. *J Biol Chem, 247*(11), 3525-3532.

Streeten, D. H., Rapoport, A., & Conn, J. W. (1963). Existence of a Slowly Exchangeable Pool of Body Sodium in Normal Subjects and Its Diminution in Patients with Primary Aldosteronism. *J Clin Endocrinol Metab, 23*, 928-937. doi:10.1210/jcem-23-9-928

Sugahara, K., & Kitagawa, H. (2000). Recent advances in the study of the biosynthesis and functions of sulfated glycosaminoglycans. *Curr Opin Struct Biol, 10*(5), 518-527.

Sureshbabu, A., Muhsin, S. A., & Choi, M. E. (2016). TGF-beta signaling in the kidney: profibrotic and protective effects. *Am J Physiol Renal Physiol, 310*(7), F596-f606. doi:10.1152/ajprenal.00365.2015

Tahara, A., Tsukada, J., Tomura, Y., Yatsu, T., & Shibasaki, M. (2008). Vasopressin increases type IV collagen production through the induction of transforming growth factor-beta secretion in rat mesangial cells. *Pharmacol Res, 57*(2), 142-150. doi:10.1016/j.phrs.2008.01.003

Tannous, B. A., Kim, D. E., Fernandez, J. L., Weissleder, R., & Breakefield, X. O. (2005). Codon-optimized Gaussia luciferase cDNA for mammalian gene expression in culture and in vivo. *Mol Ther, 11*(3), 435-443. doi:10.1016/j.ymthe.2004.10.016

Titze, J. (2014). Sodium balance is not just a renal affair. *Curr Opin Nephrol Hypertens, 23*(2), 101-105. doi:10.1097/01.mnh.0000441151.55320.c3

Titze, J., Krause, H., Hecht, H., Dietsch, P., Rittweger, J., Lang, R., . . . Hilgers, K. F. (2002). Reduced osmotically inactive Na storage capacity and hypertension in the Dahl model. *Am J Physiol Renal Physiol, 283*(1), F134-141. doi:10.1152/ajprenal.00323.2001

Titze, J., Lang, R., Ilies, C., Schwind, K. H., Kirsch, K. A., Dietsch, P., . . . Hilgers, K. F. (2003). Osmotically inactive skin Na+ storage in rats. *Am J Physiol Renal Physiol, 285*(6), F1108-1117. doi:10.1152/ajprenal.00200.2003

Titze, J., Maillet, A., Lang, R., Gunga, H. C., Johannes, B., Gauquelin-Koch, G., . . . Kirsch, K. A. (2002). Long-term sodium balance in humans in a terrestrial space station simulation study. *Am J Kidney Dis, 40*(3), 508-516. doi:10.1053/ajkd.2002.34908

Titze, J., Shakibaei, M., Schafflhuber, M., Schulze-Tanzil, G., Porst, M., Schwind, K. H., . . . Hilgers, K. F. (2004). Glycosaminoglycan polymerization may enable osmotically inactive Na+ storage in the skin. *Am J Physiol Heart Circ Physiol, 287*(1), H203-208. doi:10.1152/ajpheart.01237.2003

Trama, J., Lu, Q., Hawley, R. G., & Ho, S. N. (2000). The NFAT-related protein NFATL1 (TonEBP/NFAT5) is induced upon T cell activation in a calcineurin-dependent manner. *J Immunol, 165*(9), 4884-4894.

Urakawa, I., Yamazaki, Y., Shimada, T., Iijima, K., Hasegawa, H., Okawa, K., . . . Yamashita, T. (2006). Klotho converts canonical FGF receptor into a specific receptor for FGF23. *Nature, 444*(7120), 770-774. doi:10.1038/nature05315

Walser, M. (1985). Phenomenological analysis of renal regulation of sodium and potassium balance. *Kidney Int, 27*(6), 837-841.

Wang, W., Huang, X. R., Li, A. G., Liu, F., Li, J. H., Truong, L. D., . . . Lan, H. Y. (2005). Signaling mechanism of TGF-beta1 in prevention of renal inflammation: role of Smad7. *J Am Soc Nephrol, 16*(5), 1371-1383. doi:10.1681/asn.2004121070

Wiig, H., Schroder, A., Neuhofer, W., Jantsch, J., Kopp, C., Karlsen, T. V., . . . Titze, J. (2013). Immune cells control skin lymphatic electrolyte homeostasis and blood pressure. *J Clin Invest, 123*(7), 2803-2815. doi:10.1172/jci60113

Wolf, M. (2012). Update on fibroblast growth factor 23 in chronic kidney disease. *Kidney Int, 82*(7), 737-747. doi:10.1038/ki.2012.176

Yada, T., Gotoh, M., Sato, T., Shionyu, M., Go, M., Kaseyama, H., . . . Kimata, K. (2003). Chondroitin sulfate synthase-2. Molecular cloning and characterization of a novel human glycosyltransferase homologous to chondroitin sulfate glucuronyltransferase, which has dual enzymatic activities. *J Biol Chem, 278*(32), 30235-30247. doi:10.1074/jbc.M303657200

Yang, X. D., Zhao, L. Y., Zheng, Q. S., & Li, X. (2003). Effects of arginine vasopressin on growth of rat cardiac fibroblasts: role of V1 receptor. *J Cardiovasc Pharmacol, 42*(1), 132-135.

Zhou, X. (2016). How do kinases contribute to tonicity-dependent regulation of the transcription factor NFAT5? *World J Nephrol, 5*(1), 20-32. doi:10.5527/wjn.v5.i1.20

Ziyadeh, F. N., Sharma, K., Ericksen, M., & Wolf, G. (1994). Stimulation of collagen gene expression and protein synthesis in murine mesangial cells by high glucose is mediated by autocrine activation of transforming growth factor-beta. *J Clin Invest, 93*(2), 536-542. doi:10.1172/jci117004

6 Presentation

Poster presentation at the ERA-EDTA 55th congress, May 24th - 27th 2018 at the Bella center, Copenhagen, Denmark

ERA-EDTA: European Renal Association, European dialysis and transplant association